



European Space Agency
Agence Spatiale Européenne



director^{ate} of operations and infrastructure
ground systems engineering department
mission analysis office

MAO Working Paper No. 483
Issue 1, Rev. 0

Solar Orbiter Ballistic Transfer Mission Analysis Synthesis

by

Guy Janin and Arnaud Boutonnet

November 2005

European Space Operations Centre

Robert-Bosch-Str. 5
D - 64293 Darmstadt

PAGE INTENTIONALLY LEFT BLANK

Abstract

This Working Paper summarises mission analysis performed for the Solar Orbiter mission using chemical propulsion only. This mission is composed of a cruise phase allowing reaching a low solar orbit, followed with an inclination increase phase allowing viewing the Sun at high latitudes.

The Solar Orbiter, to be launched by a Soyuz/ST + Fregat from Kourou, performs Deep Space Manoeuvres using a monopropellant propulsion unit combined with planetary Gravity Assist Manoeuvres. An optimum transfer trajectory is calculated, leading to a 150-day orbit in a 3:2 resonance with the period of Venus and an initial perihelion radius of about 48 solar radii. During an extended part of the mission, through repeated gravity assist manoeuvres with Venus, the orbit inclination is raised without use of propulsion.

Transfer duration is 3.5 years and end of nominal mission occurs 6 years after launch. Maximum inclination in excess of 34° is reached 9.5 years after launch.

Launches during the 2013, 2015, 2017 and 2018 Venus launch window opportunity are investigated. For the 2017 launch, the planetary configuration is less favourable, the cruise phase is longer and only a 4:3 resonant orbit with Venus can be initially reached. As a consequence, the end of nominal mission occurs 7.6 years after launch.

An analysis of the navigation tasks to be performed before and after the Venus gravity assist manoeuvres during the Science phase shows that they can be performed by the AOCS at a cost of about 15 m/s per gravity assist manoeuvre.

This report, available in MS-Word and PDF format, contains colour figures.

PAGE INTENTIONALLY LEFT BLANK

Table of Content

1.	INTRODUCTION.....	1
1.1	The Solar Orbiter Mission.....	1
1.2	Mission Design.....	1
1.2.1	Transfer and Inclination Raise Phase.....	1
1.2.2	Mission Phases.....	2
2.	TRANSFER PHASE.....	3
2.1	Gravity Assist Manoeuvres.....	3
2.2	Mass Budget for Ballistic Launches in 2013 to 2018.....	3
2.3	2013 Launch.....	5
2.4	2015 Launch.....	13
2.5	2017 Launch.....	20
2.6	2018 Launch.....	28
2.7	Launch Window.....	29
3.	INCLINATION INCREASE.....	31
3.1	Procedure for Inclination Increase.....	31
3.2	Maximal Inclination Raise and Propellant Usage.....	32
4.	NAVIGATION.....	35
4.1	Introduction.....	35
4.2	Models and Assumptions.....	35
4.2.1	Spacecraft.....	35
4.2.2	Measurements.....	35
4.2.3	Covariance Analysis.....	36
4.2.4	Guidance Algorithm.....	36
4.3	Simulation Results.....	37
4.3.1	Navigation Before the Second Venus Swing-by.....	37
4.3.2	Navigation Between Second and Third Venus Swing-bys.....	40
4.4	Feasibility of the Manoeuvre Execution.....	42
4.5	Conclusion of the Navigation Analysis.....	43
5.	LAUNCHER'S PERFORMANCE.....	45
6.	CONCLUSION.....	47
7.	REFERENCES.....	49

List of Tables

Table 2-1. Ballistic mission DV and mass budget for a launch in 2013, 2015, 2017 and 2018 with a monopropellant propulsion unit with specific impulse 220 s. The spacecraft dry mass is given in the last row, column headed kg.....	4
Table 2-2. Ballistic mission timeline for a launch in 2013.	5
Table 2-3. Distance to Sun centre in AU and solar radii, spacecraft inertial orbit rotation rate and rate relative to the rotating Sun in $^{\circ}/\text{day}$ in terms of the perihelion passage number, passage date and flight time.....	8
Table 2-4. Ballistic mission timeline for a launch in 2015.	13
Table 2-5. Distance to Sun centre in AU and solar radii, spacecraft inertial orbit rotation rate and rate relative to the rotating Sun in $^{\circ}/\text{day}$ in terms of the perihelion passage number, passage date and flight time.....	16
Table 2-6. Ballistic mission timeline for a launch in 2017.	20
Table 2-7. Timeline comparison between Venus GAM 1 and 2 for the 2015 and 2017 transfer. Flight times and duration between two consecutive GAMs are in days. Last column shows the increase in duration between the 2017 and 2015 case.	21
Table 2-8. Distance to Sun centre in AU and solar radii, spacecraft inertial orbit rotation rate and rate relative to the rotating Sun in $^{\circ}/\text{day}$ in terms of the perihelion passage number, passage date and flight time.....	24
Table 2-9. Ballistic mission timeline for a launch in 2018.	28
Table 4-1. Description of the arcs analysed in this working paper. GAM V2: 2 nd Venus swing-by. GAM V3: 3 rd Venus swing-by.	35
Table 4-2. Trajectory correction manoeuvres statistics before the second Venus encounter (GAM V2).....	37
Table 4-3. Evolution of the 1σ dispersion covariance matrix at pericentre projected on the target plane (GAM V2).	38
Table 4-4. Trajectory correction manoeuvres statistics between the second and the third Venus (GAM V3).	40
Table 4-5. Evolution of the 1σ dispersion covariance matrix at pericentre projected on the target plane (GAM V3).	40

Table of Figures

Figure 2-1. Ballistic transfer, 2013 launch: ecliptic view of the trajectory, GAMs until Venus GAM 2 and DSM.	6
Figure 2-2. Ballistic transfer, 2013 launch: projection of the trajectory on the ecliptic system (y, z)-plane.....	7
Figure 2-3. Ballistic transfer, 2013 launch: projection of the trajectory on the ecliptic system (x, z)-plane.....	7
Figure 2-4. Ballistic transfer, 2013 launch: distance of the spacecraft from Earth, Venus and Sun function of flight day.	9
Figure 2-5. Ballistic transfer, 2013 launch: angle Sun-Spacecraft-Earth and Sun-Earth-Spacecraft and distance to Sun centre [AU] function of flight day.....	9
Figure 2-6. Ballistic transfer, 2013 launch: solar latitude function of flight day.	10
Figure 2-7. Ballistic transfer, 2013 launch: solar latitude function of distance Spacecraft-Sun.....	10
Figure 2-8. Ballistic transfer, 2013 launch: solar radiation integrated doses function of flight day. .	11
Figure 2-9. Ballistic transfer, 2013 launch: velocity toward the Sun [km/s] and distance to Sun centre during first revolution after Venus GAM 2.....	11
Figure 2-10. Ballistic transfer, 2013 launch: velocity rate toward the Sun [mm/s^2] and distance to Sun centre during first revolution after Venus GAM 2.	12
Figure 2-11. Ballistic transfer, 2013 launch: coverage in hours/day from New Norcia function of flight day.	12
Figure 2-12. Ballistic transfer, 2013 launch: coverage in hours/day from Cebreros function of flight day.	13
Figure 2-13. Ballistic transfer, 2015 launch: ecliptic view of the trajectory, GAMs until Venus GAM 2 and DSMs.	14
Figure 2-14. Ballistic transfer, 2015 launch: projection of the trajectory on the ecliptic system (y, z)-plane.....	15
Figure 2-15. Ballistic transfer, 2015 launch: projection of the trajectory on the ecliptic system (x, z)-plane.....	15
Figure 2-16. Ballistic transfer, 2015 launch: distance of the spacecraft from Earth, Venus and Sun function of flight day.	17
Figure 2-17. Ballistic transfer, 2015 launch: angle Sun-Spacecraft-Earth and Sun-Earth-Spacecraft and distance to Sun centre [AU] function of flight day.....	17
Figure 2-18. Ballistic transfer, 2015 launch: solar latitude function of flight day.	18
Figure 2-19. Ballistic transfer, 2015 launch: solar latitude function of distance Spacecraft-Sun.	18
Figure 2-20. Ballistic transfer, 2015 launch: solar radiation integrated doses function of flight day.	19
Figure 2-21. Ballistic transfer, 2015 launch: coverage in hours/day from New Norcia function of flight day.	19

Figure 2-22. Ballistic transfer, 2015 launch: coverage in hours/day from Cebreros function of flight day.	20
Figure 2-23. Ballistic transfer, 2017 launch: ecliptic view of the trajectory, GAMs until Venus GAM 2 and DSMs.	22
Figure 2-24. Ballistic transfer, 2017 launch: projection of the trajectory on the ecliptic system (y, z)-plane.	23
Figure 2-25. Ballistic transfer, 2017 launch: projection of the trajectory on the ecliptic system (x, z)-plane.	23
Figure 2-26. Ballistic transfer, 2017 launch: distance of the spacecraft from Earth, Venus and Sun function of flight day.	25
Figure 2-27. Ballistic transfer, 2017 launch: angle Sun-Spacecraft-Earth and Sun-Earth-Spacecraft and distance to Sun centre [AU] function of flight day.	25
Figure 2-28. Ballistic transfer, 2017 launch: solar latitude function of flight day.	26
Figure 2-29. Ballistic transfer, 2017 launch: solar latitude function of distance Spacecraft-Sun.	26
Figure 2-30. Ballistic transfer, 2017 launch: solar radiation integrated doses function of flight day.	27
Figure 2-31. Ballistic transfer, 2017 launch: coverage in hours/day from New Norcia function of flight day.	27
Figure 2-32. Ballistic transfer, 2017 launch: coverage in hours/day from Cebreros function of flight day.	28
Figure 2-33. Variation in escape velocity and total DSM DV for optimum launches between May 8 and June 4, 2015.	29
Figure 3-1. Relation between perihelion radius and planar Venus hyperbolic arrival velocity for a 3:2 resonant orbit with Venus.	31
Figure 3-2. Arrival hyperbolic velocity at Venus GAM 2 in terms of reachable final inclination with respect to solar equator for the 2013 ballistic mission.	32
Figure 3-3. Δ -monopropellant mass in terms of the reachable final inclination relative to the solar equator for a CP mission.	33
Figure 4-1. Evolution of the 1σ position knowledge (thick lines) and dispersion (thin lines) mapped to the pericentre (GAM V2).	38
Figure 4-2. Evolution of the 1σ velocity knowledge (thick lines) and dispersion (thin lines) mapped to the pericentre (GAM V2).	39
Figure 4-3. Dispersion 1σ ellipses at pericentre of the second Venus gravity assist (GAM V2).	39
Figure 4-4. Evolution of the 1σ position knowledge (thick lines) and dispersion (thin lines) mapped to the pericentre (GAM V3).	41
Figure 4-5. Evolution of the 1σ velocity knowledge (thick lines) and dispersion (thin lines) mapped to the pericentre (GAM V3).	41
Figure 4-6. Dispersion 1σ ellipse at pericentre of the second Venus gravity assist (GAM V3).	42
Figure 5-1. Soyuz/ST + Fregat performance (kg, including adapter) for highly elliptic (perigee height 200 km) and escape missions in terms of C_3 for a launch from Kourou with inclination $i = 5^\circ$, 28.5° , 51.8° and 64.9° (Ref. 3).	45

Figure 5-2. Correspondence between C_3 and apogee height (black curve) and perigee injection DV (blue curve).....46

Index of Abbreviations

AU	Astronomical Unit
AOCS	Attitude and Orbit Control System
CP	Chemical Propulsion
C_r	Radiation pressure coefficient
C_3	Square of the hyperbolic excess velocity
DSM	Deep Space Manoeuvre
ΔV	Velocity increment
ENM	End of Nominal Mission
EOM	<u>E</u> nd of <u>m</u> ission (end of further extended mission)
ESA	European Space Agency
ESOC	European Space Operations Centre
EXM	<u>E</u> nd of <u>e</u> xtended <u>m</u> ission
GA	Gravity Assist
GAM	Gravity Assist Manoeuvre
GNC	Guidance, Navigation and Control
HQ	<u>H</u> ead <u>q</u> uarter
i.e.	Id est
LQC	Linear Quadratic Control
LSO	Low Solar Orbit
LTF	Linear Time of Flight
LW	Launch Window
MAO	Mission Analysis Office
MLS	Minimum Least Square
PMSL	Passage at Maximum Solar Latitude
R_E	Earth Radius
SMAA	<u>S</u> emi- <u>m</u> ajor <u>a</u> xis
SMIA	<u>S</u> emi- <u>m</u> inor <u>a</u> xis
SOHO	<u>S</u> olar and <u>H</u> eliospheric <u>O</u> bservatory
SR	Solar Radius
TCM	Trajectory Correction Manoeuvre
V_{inf}	Infinite velocity or hyperbolic excess velocity or asymptotic velocity or escape velocity
WP	Working Paper
w.r.t.	With respect to

1. INTRODUCTION

1.1 *The Solar Orbiter Mission*

The Sun's atmosphere and the heliosphere represent uniquely accessible domains of space, where fundamental physical processes common to solar, astrophysical and laboratory plasmas can be studied in detail and under conditions impossible to reproduce on Earth or to study from astronomical distances.

The results from missions such as Ulysses and SOHO have advanced enormously our understanding of the solar corona, the associated solar wind and the three-dimensional heliosphere. However, we have reached the point where further in-situ measurements, now much closer to the Sun, together with high-resolution imaging and spectroscopy from a near-Sun and out-of-ecliptic perspective, promise to bring about major breakthroughs in solar and heliospheric physics.

The Solar Orbiter will for the first time

- ✓ explore the uncharted innermost regions of our solar system,
- ✓ study the Sun from close-up (48-50 solar radii, about 0.22 AU),
- ✓ fly by the Sun and examine the solar surface and the space above from a nearly co-rotating vantage point,
- ✓ provide images of the Sun's polar regions from heliographic latitudes as high as 35°.

1.2 *Mission Design*

1.2.1 **Transfer and Inclination Raise Phase**

Using planetary gravity assist manoeuvres with Venus and Earth and Deep Space Manoeuvres (DSM) with Chemical Propulsion (CP), an orbit with a perihelion between 48 and 50 solar radii and a period of about 150 days will be achieved after a transfer lasting about 3.5 years. Then, adjusting the orbit period such that it is commensurable with the period of the orbit of Venus will cause a succession of high energy Venus encounters allowing to gradually increase the inclination of the orbit. About 9 years after launch the orbit inclination relative to the solar equator will reach a value close to 35°.

The last Venus swing-by will aim to a non-resonant orbit assuring that the spacecraft will not crash on the planet at next encounter. By a proper selection of the swing-by parameters, an orbit with lower perihelion radius can be achieved again, without reduction of the inclination.

Launch is foreseen from Kourou with a Soyuz/ST version 2-1b equipped with a Fregat upper stage.

Interplanetary transfers are calculated with the help of an optimisation program. Cost function is maximum mass at arrival on the low perihelion orbit. For the Solar Orbiter mission a second quantity is to be maximised: the inclination reached at the end of the inclination raise sequence. In addition the transfer and inclination raise phase duration have to be minimised. Constraints are:

1. Minimum altitude above planet surface during swing-bys (300 km)

2. Minimum perihelion distance to the Sun (0.22 AU)
3. No manoeuvre below distance 0.6 AU from the Sun

Calculation of the spacecraft mass at end of transfer has to take into account

1. Performance of the launcher
2. Provision for a launch window
3. Launcher dispersion correction
4. DSMs
5. Navigation DV
6. Overall margin

In this report,

- Launcher performance is defined by a table of useful mass in terms of injection orbit energy
- Interplanetary ballistic arcs are approximated by Kepler arcs
- A link conic approximation is used for calculating planetary swing-bys, which are therefore considered as impulsive manoeuvres
- DSMs performed by CP are considered as impulsive (thrusters are only defined by their specific impulse).

For interplanetary mission design, errors resulting from such approximations are very small and feasibility of the mission is fully warranted.

1.2.2 Mission Phases

The Solar Orbiter mission is divided into three phases:

1. Nominal mission ending at End of Nominal Mission (ENM)
2. Extended mission ending at End of eXtended Mission (EXM)
3. Further extended mission ending at End Of Mission (EOM).

The end of a phase is defined when a given science goal has been reached. For the Solar Orbiter the passage over the north pole of the Sun being a major observational event the end of a phase will occur after such event. The precise date when a phase ends depends on the time to downlink telemetry generated before and during the passage. The duration of this operation depends on on-board memory usage and telemetry rate, which is function of the distance to the Earth. Therefore, for each mission (launch year) end-of-phase dates are estimated individually. Generally, the

- ENM is defined after the fourth encounter with Venus during the inclination raise phase when orbiting on a resonant orbit with Venus. At this time the orbit inclination relative to the solar equator has reached a value already larger than 20° ,
- EXM is defined after Venus GAM 6, when the inclination is close to its maximum attainable value,
- EOM follows GAM 7, after staying about three revolutions on a non-resonant orbit, targeted so that the maximum obtainable value for the inclination is reached, or alternately, the perihelion radius is again reduced (see Section 3.1).

2. TRANSFER PHASE

2.1 Gravity Assist Manoeuvres

Deviation of the velocity vector of a spacecraft relative to a massive body (planet) due to a close encounter with this body allows a change of the spacecraft's orbit parameters relative to the central body (Sun). The close encounter is called *swing-by* and the change of the orbit parameters is equivalent to a manoeuvre, called *Gravity Assist Manoeuvre (GAM)*. A swing-by becomes just a *fly-by* when the massive body is small (asteroid, comet nucleus) and no sizeable deviation of the velocity vector is obtained.

GAMs can be performed in such a way as to change the orbital energy of the spacecraft (actually the energy is borrowed from the massive body) without propellant expense. The price to pay is:

- Reduction of mission design flexibility
- Increase of mission duration
- Increase of operations complexity
- Increase of mission failure risk

In spite of these drawbacks, GAMs have been very popular in interplanetary mission design. Therefore, they are also considered for the Solar Orbiter mission.

The most effective planet for GAM is Jupiter. It has been used with success for sending the Ulysses solar polar observer on the desired out of ecliptic trajectory (80° inclination to the ecliptic plane). However, the following drawbacks in the mission design had to be accepted:

- Long mission time (4 years up to first solar polar pass)
- High energy requirement to reach Jupiter (11.4 km/s for Ulysses) or increased mission time if GAMs by terrestrial planets are used to reduce the energy requirement
- High aphelion of the resulting solar orbit (5 AU)
- Very high period of revolution around the Sun (6.2 years)

Therefore, such a Jupiter GAM will not be considered for the Solar Orbiter.

The other planets entering into consideration are Mars, Earth, Venus and Mercury. Mars will be excluded because its use leads to too long mission duration and Mercury, due to its small mass, is of little interest for GAM.

2.2 Mass Budget for Ballistic Launches in 2013 to 2018

A ballistic transfer is an interplanetary transfer making use of GAMs and impulsive DSMs. One of the main output of this mission analysis document is the *DV* budget for manoeuvres. By applying the rocket equation a mass budget can be estimated. The *DV* budget is based on the following considerations:

1. **Escape velocity:** an optimum balance between the use of the launcher's injection capability and the spacecraft on-board propulsion unit has to be reached. This is achieved by including launcher's performance into the overall trajectory optimisation.

2. **Launcher performance:** a launcher performance curve in terms of the hyperbolic excess velocity or its square (escape energy C_3 , see Figure 5-1) is required for the trajectory optimisation program.
3. **Launch window:** to provide for a seasonal Launch Window (LW) a certain performance margin is to be included.
4. **Correction of launcher dispersion:** such a correction, of the order of 30 m/s, is accomplished after the first orbit determination on the escape orbit, two or three days after launch.
5. **DSM DV:** output of the trajectory optimisation.
6. **GAM preparation/correction and navigation:** a certain provision for it is to be added to the DV requirement.
7. **Overall margin:** a given percentage of the total DV is added.

The first planet used for a GAM is Venus. Optimum launch periods are therefore tied to the Venus LWs, occurring every 19 months.

Such windows along years 2013 to 2018 were explored and a corresponding optimum transfer trajectory was found.

Transfers.- For 2013, 2015 and 2018 launches, short transfers of about 3.4 years are available. For 2017, the transfer is longer (4.1 years). The 2013, 2015 and 2017 cases are described in more details in Sections 2.3 to 2.5. A mission timeline for a 2018 launch is given in Section 2.6.

Launch window penalty.- To allow for a LW, namely a launch before/after the optimum launch date, a certain performance penalty has to be foreseen. This is investigated in Section 2.5, which shows that such a penalty is of the order of 130 m/s on the escape velocity and 58 m/s on the DSM for allowing a 3-week window. This figure will be taken as typical LW penalty.

Mass budget.- Using launcher's performance (Chap. 5) and the various DV requirements, Table 2-1 gives the corresponding mass budget for a monopropellant propulsion system with a specific impulse of 220 s. The mass listed in the bottom row is the spacecraft dry mass at End Of Mission (EOM), taking navigation requirement for all the GAMs. In these calculations the launcher adapter is assumed to be a fixed part of the spacecraft.

Solar Orbiter Ballistic Missions 2013-2018								
	2013		2015		2017		2018	
	km/s	kg	km/s	kg	km/s	kg	km/s	kg
Escape Vinf	3.522	1356	3.557	1345	3.538	1351	3.436	1382
LW delta-Vinf	0.130	1315	0.130	1304	0.130	1310	0.130	1342
Dispersion launcher	0.030	1297	0.030	1286	0.030	1292	0.030	1323
Total DSM	0.277	1141	0.077	1241	0.000	1292	0.174	1221
LW delta-DSM	0.058	1111	0.058	1208	0.058	1258	0.058	1189
Navigation	0.135	1043	0.135	1135	0.135	1181	0.135	1116
Overall 5 % margin	0.032	1028	0.022	1124	0.018	1172	0.026	1103

Table 2-1. Ballistic mission DV and mass budget for a launch in 2013, 2015, 2017 and 2018 with a monopropellant propulsion unit with specific impulse 220 s. The spacecraft dry mass is given in the last row, column headed kg.

2.3 2013 Launch

For the nominal 2013 launch, the following results and considerations are in order:

1. The optimum balance between the use of the launcher's injection capability and the spacecraft on-board propulsion unit leads to the selection of an escape velocity of 3.522 km/s to be provided by the launcher.
2. Corresponding Soyuz/ST performance is 1356 kg (see performance curve in Chap. 5). In this analysis, the mass of the adapter is assumed to be part of the spacecraft dry mass.
3. Penalty on the launcher performance for allowing a 3-week LW is estimated to be 130 m/s (Section 2.7), resulting in a usable Soyuz/ST performance of 1315 kg.
4. Correction of the launcher dispersion amounts to 30 m/s.
5. There is only one DSM with a DV of 277 m/s. To this, 58 m/s has to be added as a penalty for the LW. DSMs will be performed with the AOCS with an assumed specific impulse of 220 s.
6. DV usage for preparation and correction of GAMs and navigation is estimated to be 15 m/s per GAM and will be performed with the AOCS (see Chap. 4). The navigation cost of 135 m/s results from a total of 9 GAMs. This includes a 7th Venus GAM, to be possibly performed after the End of eXtended Mission (EXM).
7. Finally, an overall margin corresponding to 5 % of the total DV is added.

The mass budget table is shown in Table 2-1 columns headed 2013.

The timeline for an optimum transfer in 2013 is shown in Table 2-2. In addition to flight time, inclination relative to the ecliptic plane and the solar equator, aphelion and perihelion radius in AU are listed.

Date	Flight time		Event	Inclination [°]		Aphelion [AU]	Perihelion	
	Days	Years		Ecliptic	Sol. equ.		[AU]	[Sol. rad.]
2013-10-23	0	0	Launch	1.3	6.4	0.999	0.678	146
2014-04-24	182	0.50	GAM V1	1.2	7.1	1.379	0.725	156
2014-10-10	351	0.96	DSM 1	1.2	7.1	1.379	0.725	156
2015-03-06	499	1.37	GAM E1	0.0	7.3	1.104	0.463	100
2016-12-29	1163	3.18	GAM E2	4.1	3.8	0.990	0.294	63
2017-03-04	1228	3.36	GAM V2	5.2	7.0	0.880	0.224	48
2018-05-30	1679	4.60	GAM V3	14.5	16.4	0.860	0.244	53
2019-08-20	2127	5.82	GAM V4	22.5	24.4	0.822	0.282	61
2019-11-27	2226	6.09	ENM	22.5	24.4	0.822	0.282	61
2020-11-11	2576	7.05	GAM V5	28.1	30.0	0.775	0.329	71
2022-02-04	3025	8.28	GAM V6	31.3	33.1	0.733	0.371	80
2022-05-29	3139	8.60	EXM	31.3	33.1	0.733	0.371	80
2023-04-29	3475	9.51	GAM V7	32.1	34.0	0.719	0.385	83
2024-06-29	3902	10.68	EOM	32.1	34.0	0.719	0.385	83

Table 2-2. Ballistic mission timeline for a launch in 2013.

First Passage at Maximum Solar Latitude (PMSL) after Venus GAM 4 occurs on 2019-10-26 and ENM is defined one month later, on 2019-11-27. EXM is defined on 2022-05-29, about four weeks

after first PMSL following GAM 6 on 2022-05-03. Finally, EOM is defined on 2024-06-29, after three PMSLs following GAM 7.

Trajectory plots.- Figure 2-1 shows the projection of the trajectory on the ecliptic plane and symbols represent DSM and GAMs until Venus GAM 2. Figure 2-2 and Figure 2-3 show the projection of the trajectory on the ecliptic system (y, z)-plane and (x, z)-plane respectively.

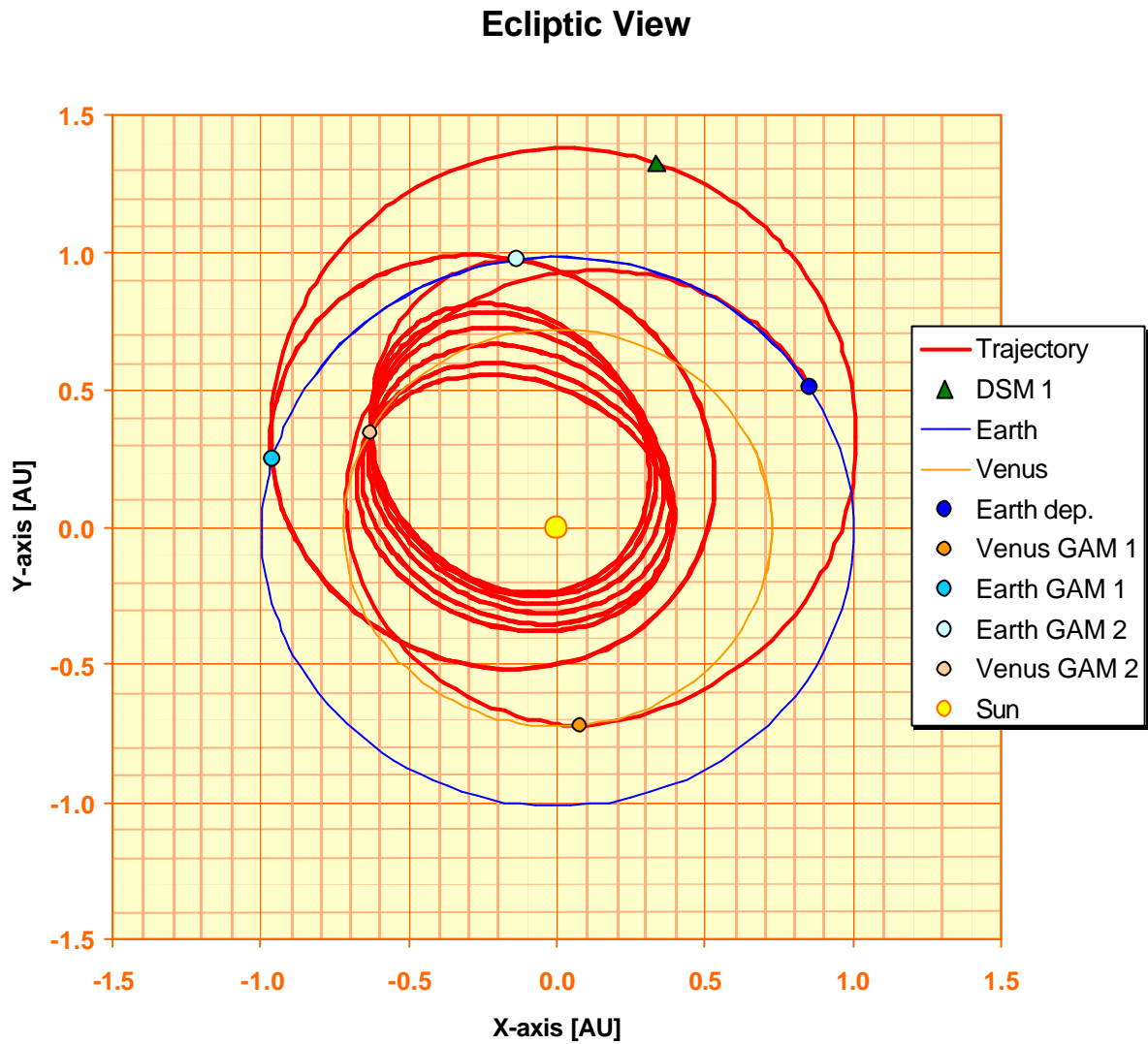


Figure 2-1. Ballistic transfer, 2013 launch: ecliptic view of the trajectory, GAMs until Venus GAM 2 and DSM.

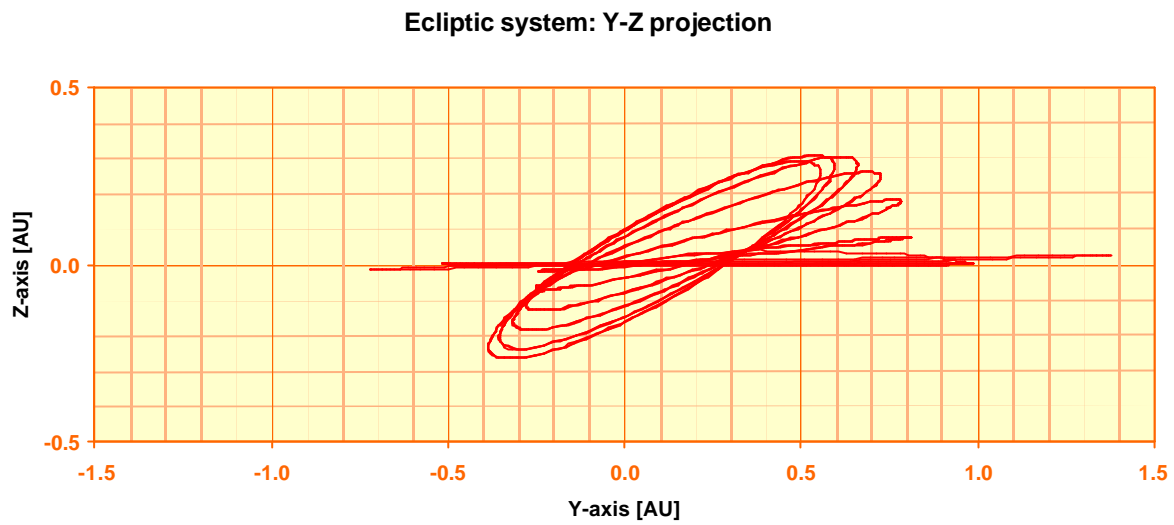


Figure 2-2. Ballistic transfer, 2013 launch: projection of the trajectory on the ecliptic system (y, z)-plane.

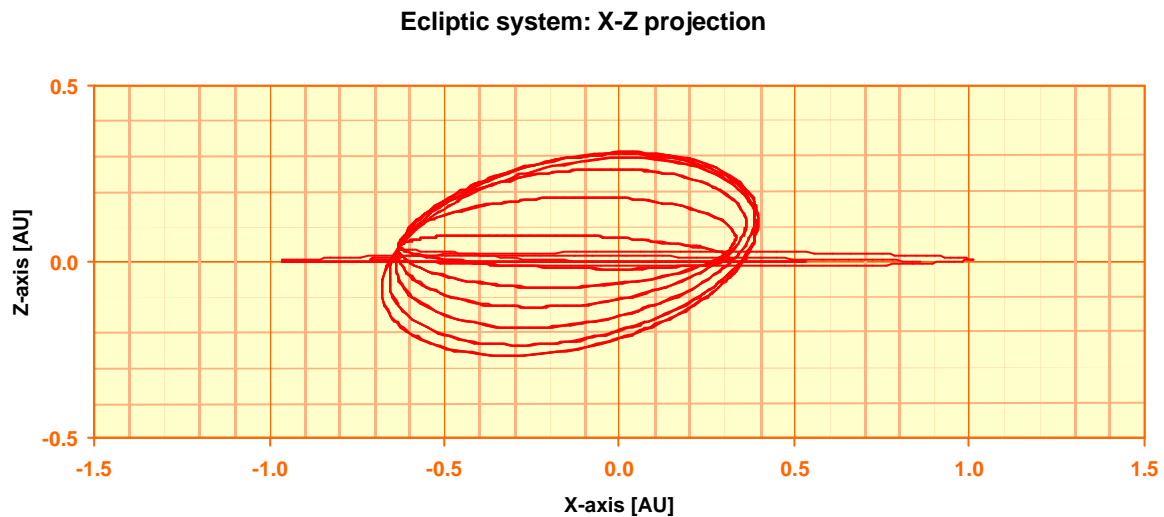


Figure 2-3. Ballistic transfer, 2013 launch: projection of the trajectory on the ecliptic system (x, z)-plane.

For each perihelion passage, Table 2-3 lists the distance to Sun centre in AU and solar radii, the spacecraft inertial orbit rotation rate (angular rate of the true anomaly) and rate relative to the rotating Sun in $^{\circ}/\text{day}$ in terms of the perihelion passage date and flight time.

Perihelion number	Date Perihelion	Flight time		Dist. to Sun		Rate [°/d]	
		Days	Years	[AU]	[SR]	inertial	/Sun
PER 1	2014-03-25	152	0.42	0.678	146	1.9	-12.3
PER 2	2015-05-24	578	1.58	0.463	100	3.7	-10.5
PER 3	2016-02-01	831	2.27	0.463	100	3.7	-10.5
PER 4	2016-10-13	1086	2.97	0.463	100	3.7	-10.5
PER 5	2017-04-11	1266	3.47	0.224	48	11.6	-2.5
PER 6	2017-09-08	1416	3.88	0.224	48	11.6	-2.5
PER 7	2018-02-05	1566	4.29	0.225	48	11.6	-2.6
PER 8	2018-07-07	1717	4.70	0.244	53	10.1	-4.0
PER 9	2018-12-04	1867	5.11	0.245	53	10.1	-4.1
PER 10	2019-05-03	2017	5.52	0.245	53	10.1	-4.1
PER 11	2019-10-03	2171	5.94	0.282	61	8.0	-6.2
PER 12	2020-03-01	2321	6.35	0.282	61	8.0	-6.2
PER 13	2020-07-29	2471	6.76	0.282	61	8.0	-6.2
PER 14	2021-01-01	2627	7.19	0.329	71	6.2	-8.0
PER 15	2021-05-31	2777	7.60	0.329	71	6.2	-8.0
PER 16	2021-10-28	2927	8.01	0.329	71	6.2	-8.0
PER 17	2022-04-07	3087	8.45	0.371	80	5.0	-9.2
PER 18	2022-09-04	3237	8.86	0.371	80	5.0	-9.2
PER 19	2023-02-01	3387	9.27	0.371	80	5.0	-9.2
PER 20	2023-07-11	3548	9.71	0.385	83	4.7	-9.5
PER 21	2023-12-08	3698	10.12	0.385	83	4.7	-9.5
PER 22	2024-05-05	3847	10.53	0.385	83	4.7	-9.5

Table 2-3. Distance to Sun centre in AU and solar radii, spacecraft inertial orbit rotation rate and rate relative to the rotating Sun in °/day in terms of the perihelion passage number, passage date and flight time.

Parameter plots.- The following set of diagrams (Figure 2-4 to Figure 2-8) show

1. The distance in AU of the spacecraft from Earth, Venus and Sun function of flight time in days.
2. The angle Sun-Spacecraft-Earth and Sun-Earth-Spacecraft and the distance of the spacecraft to the Sun [AU] function of flight time in days.
3. The solar latitude function of flight time in days.
4. The solar latitude of the subsatellite point in terms of the distance of the spacecraft to the Sun [AU].
5. The solar radiation integrated doses function of flight time in days.

The solar radiation integrated doses is a non-dimensional figure defined as the solar radiation doses normalised at 1 AU along a unit of time divided by the flight time. It is proportional to the total (cumulated) doses of solar radiation received by the spacecraft during the flight.

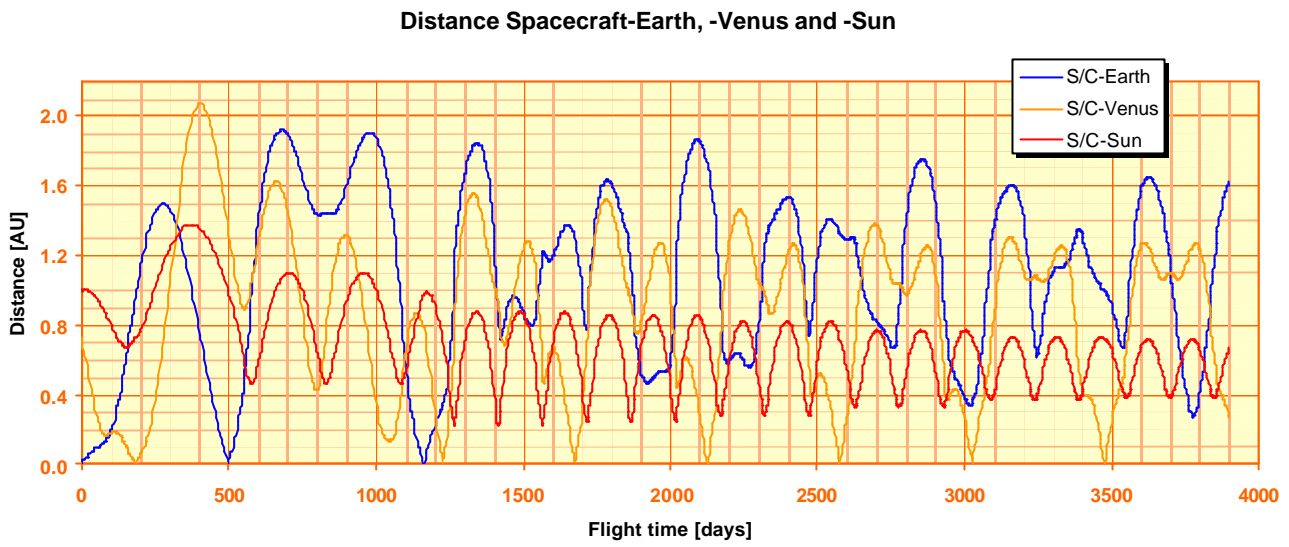


Figure 2-4. Ballistic transfer, 2013 launch: distance of the spacecraft from Earth, Venus and Sun function of flight day.

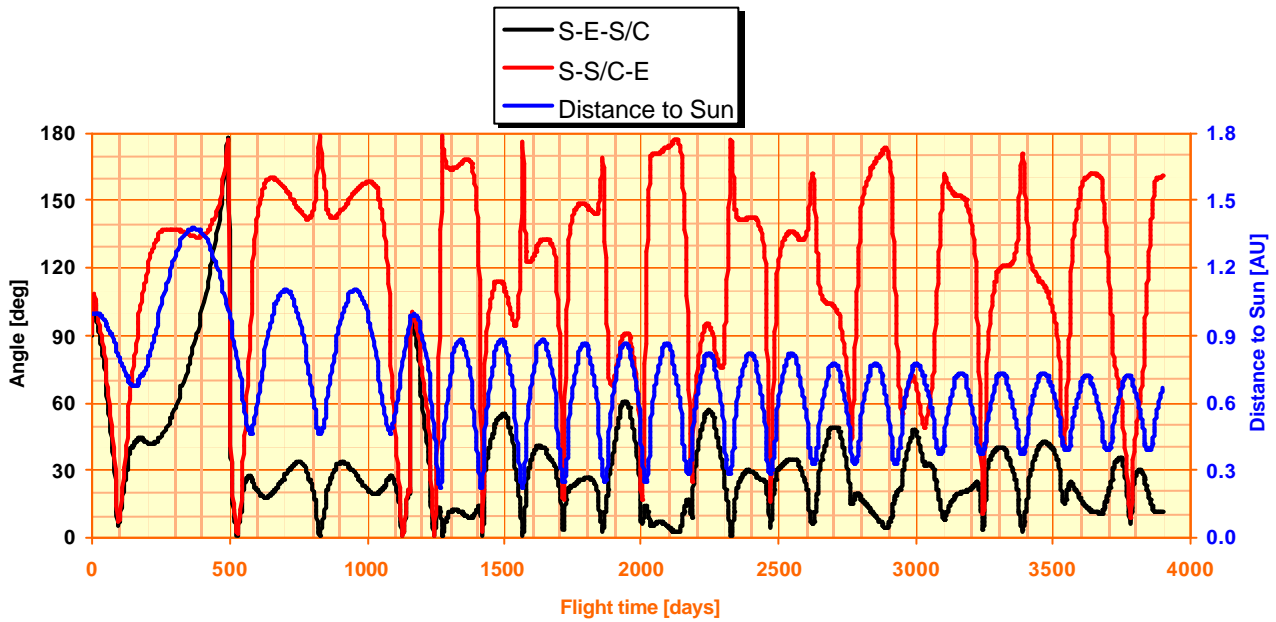


Figure 2-5. Ballistic transfer, 2013 launch: angle Sun-Spacecraft-Earth and Sun-Earth-Spacecraft and distance to Sun centre [AU] function of flight day.

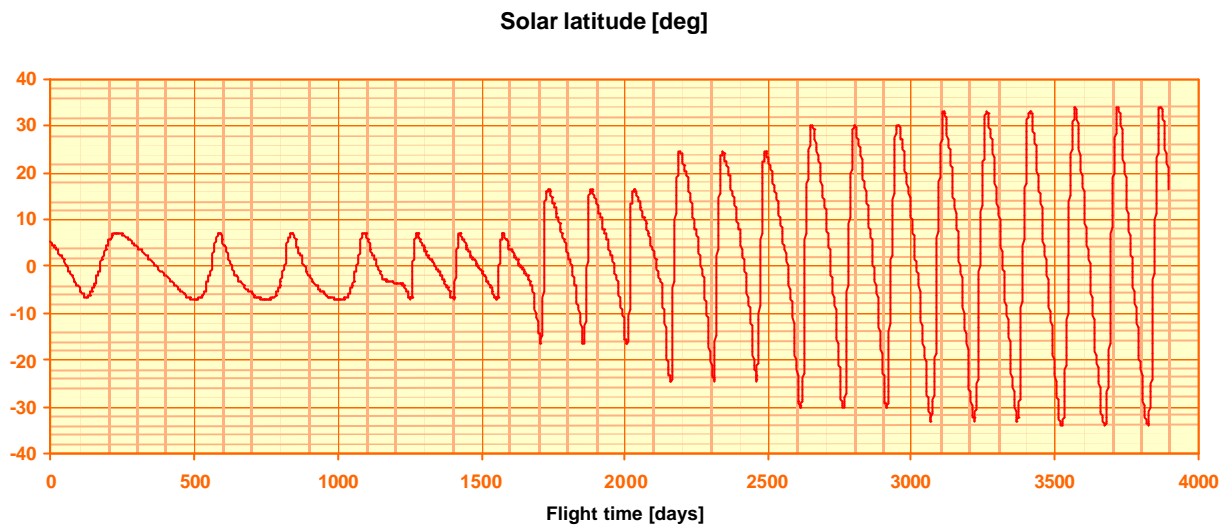


Figure 2-6. Ballistic transfer, 2013 launch: solar latitude function of flight day.

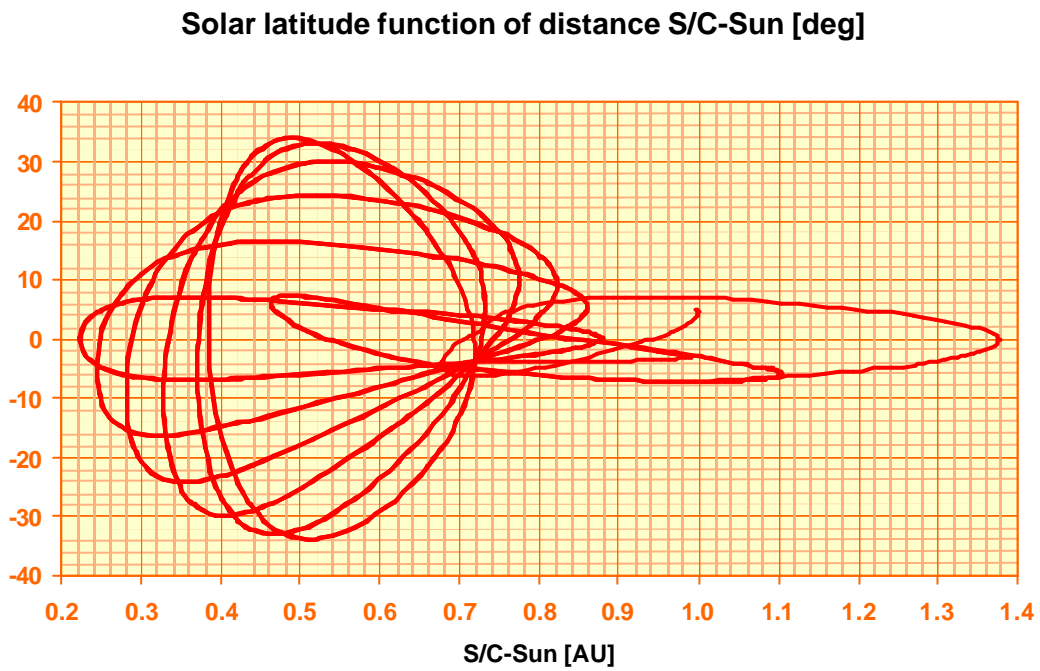


Figure 2-7. Ballistic transfer, 2013 launch: solar latitude function of distance Spacecraft-Sun.

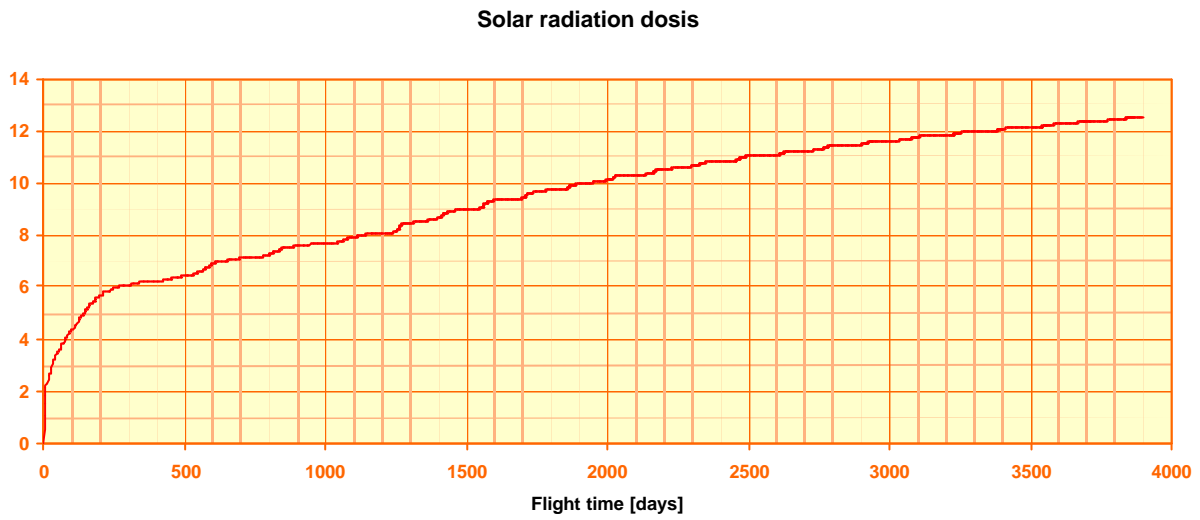


Figure 2-8. Ballistic transfer, 2013 launch: solar radiation integrated doses function of flight day.

Radial velocity toward the Sun and its rate during the first revolution after Venus GAM 2 are shown respectively on Figure 2-9 and Figure 2-10.

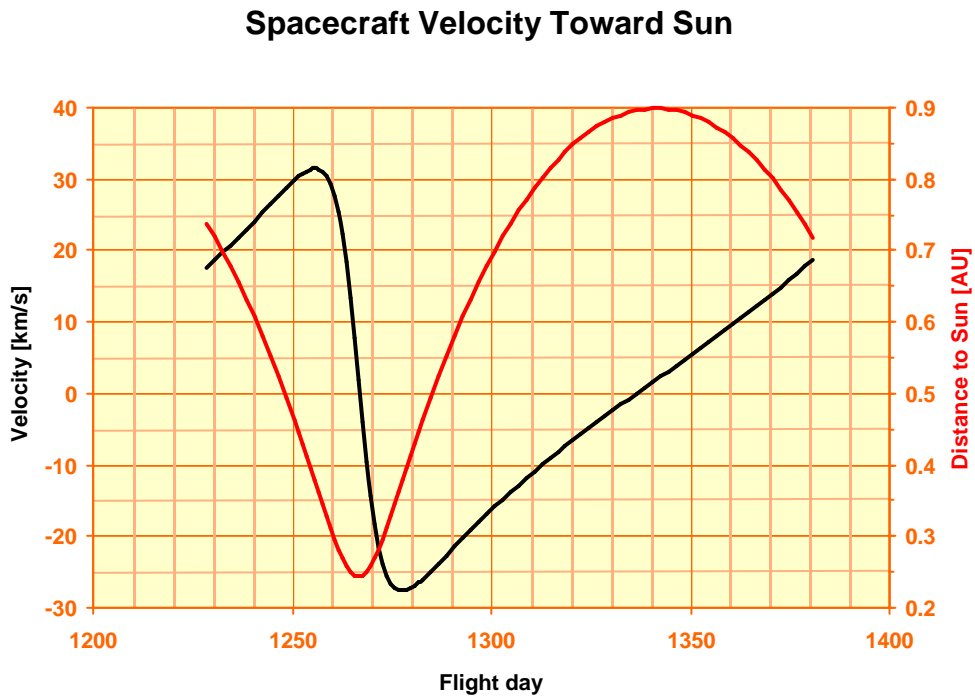


Figure 2-9. Ballistic transfer, 2013 launch: velocity toward the Sun [km/s] and distance to Sun centre during first revolution after Venus GAM 2.

Spacecraft Velocity Rate Toward Sun

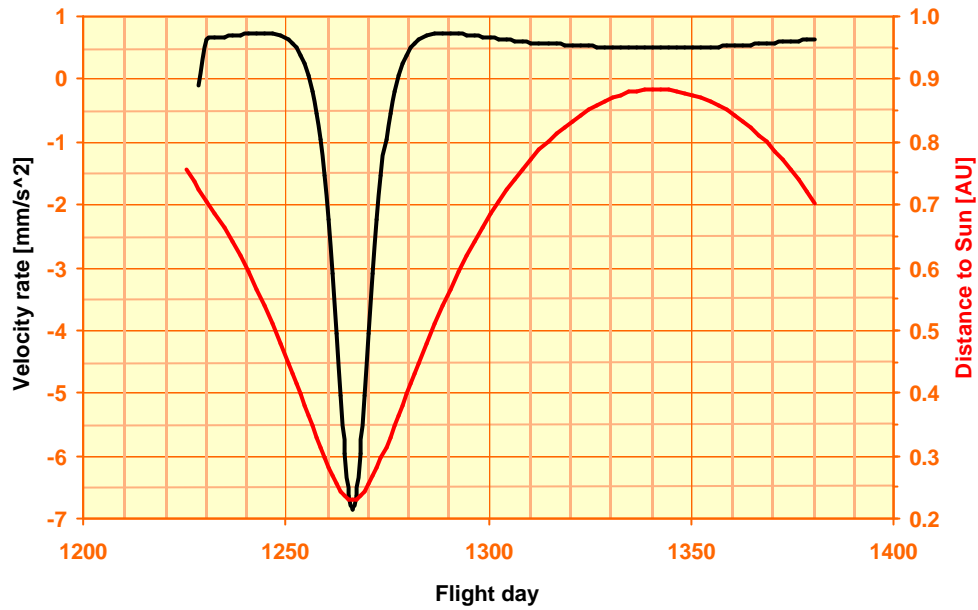


Figure 2-10. Ballistic transfer, 2013 launch: velocity rate toward the Sun [mm/s^2] and distance to Sun centre during first revolution after Venus GAM 2.

Finally, coverage in hours/day from station New Norcia (long. 116.20° , lat. -30.97°) and Cebreros (long. -4.36° , lat. 40.45°) is shown respectively on Figure 2-11 and Figure 2-12 for 10° and 30° minimum elevation.

New Norcia coverage in hours/day

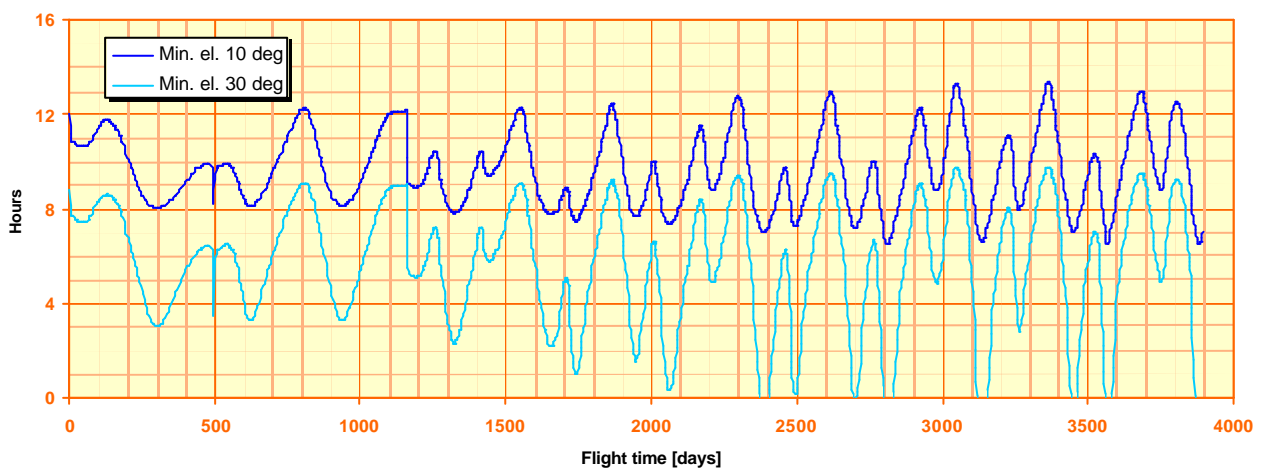


Figure 2-11. Ballistic transfer, 2013 launch: coverage in hours/day from New Norcia function of flight day.

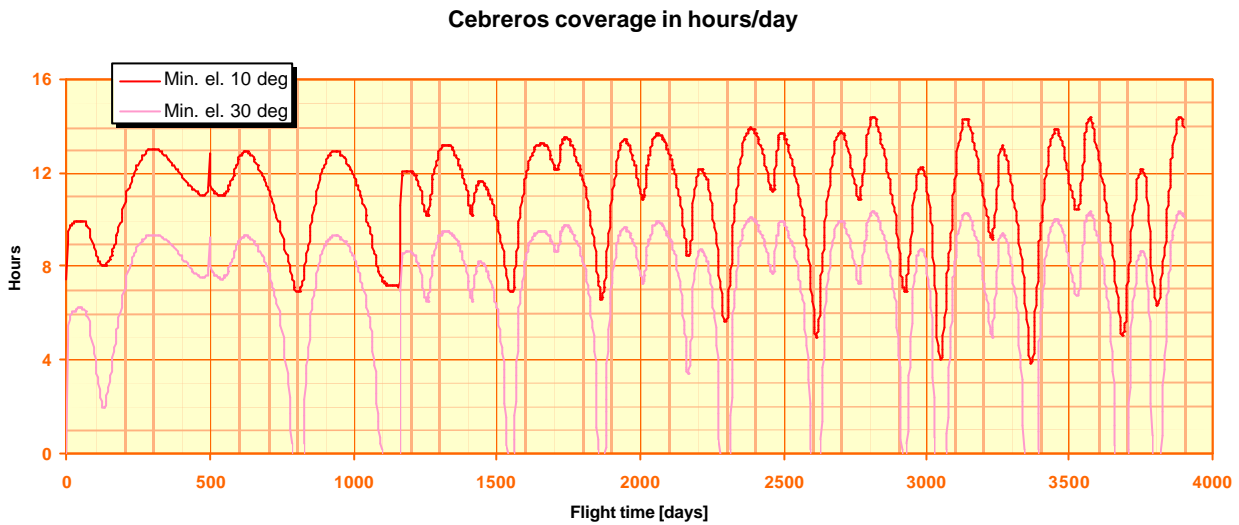


Figure 2-12. Ballistic transfer, 2013 launch: coverage in hours/day from Ceberos function of flight day.

2.4 2015 Launch

The mass budget table for a 2015 ballistic mission is shown in Table 2-1 columns headed 2015. While the escape velocity is slightly higher for the 2015 launch than for 2013 (3.557 versus 3.522 km/s), the total DSM is much lower (77 versus 277 m/s) allowing a spacecraft dry mass almost 100 kg higher.

The mission timeline for an optimum transfer in 2015 is shown in Table 2-4. The timeline is very similar to the 2013 launch, except the DSM, scheduled after Venus GAM 1 instead of before.

Date	Flight time		Event	Inclination [°]		Aphelion [AU]	Perihelion	
	Days	Years		Ecliptic	Sol. equ.		[AU]	[Sol. rad.]
2015-05-22	0	0	Launch	2.9	4.5	1.022	0.674	145
2015-11-26	188	0.51	GAM V1	2.8	6.3	1.384	0.716	154
2016-05-28	372	1.02	DSM 1	2.8	6.3	1.384	0.708	152
2016-10-08	505	1.38	GAM E1	0.0	7.3	1.101	0.460	99
2018-08-08	1174	3.21	GAM E2	4.1	6.3	1.015	0.305	66
2018-10-09	1236	3.39	GAM V2	8.0	10.5	0.879	0.225	48
2020-01-02	1686	4.62	GAM V3	17.4	20.0	0.852	0.252	54
2021-03-26	2135	5.85	GAM V4	24.7	27.3	0.809	0.295	63
2021-07-08	2239	6.13	ENM	24.7	27.3	0.809	0.295	63
2022-06-19	2585	7.08	GAM V5	29.4	31.9	0.762	0.342	74
2023-09-11	3034	8.31	GAM V6	31.5	34.0	0.729	0.375	81
2024-01-31	3176	8.70	EXM	31.5	34.0	0.729	0.375	81
2024-12-03	3483	9.54	GAM V7	31.6	34.2	0.726	0.378	81
2026-02-25	3932	10.77	EOM	31.6	34.2	0.726	0.378	81

Table 2-4. Ballistic mission timeline for a launch in 2015.

First PMSL after Venus GAM 4 occurs on 2021-06-12 and ENM is defined four weeks later, on 2021-07-08. EXM is defined on 2024-01-31, about six weeks after first PMSL following GAM 6 on 2023-12-18. Finally, EOM is defined on 2026-02-25, after three PMSLs following GAM 7.

Figure 2-13 shows the projection of the trajectory on the ecliptic plane and symbols represent DSMs and GAMs until Venus GAM 2. Figure 2-14 and Figure 2-15 show the projection of the trajectory on the ecliptic system (y, z)-plane and (x, z)-plane respectively.

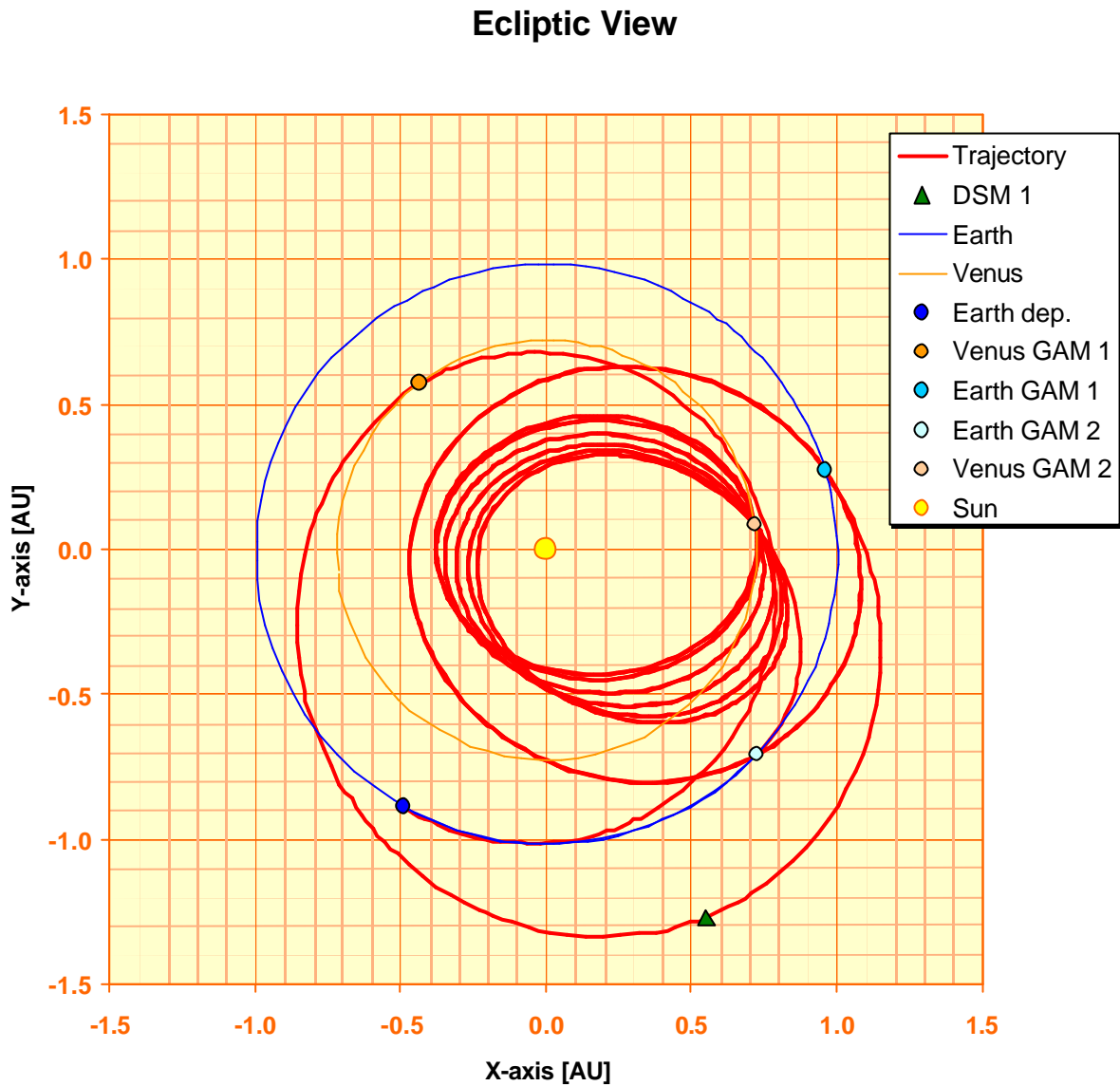


Figure 2-13. Ballistic transfer, 2015 launch: ecliptic view of the trajectory, GAMs until Venus GAM 2 and DSMs.

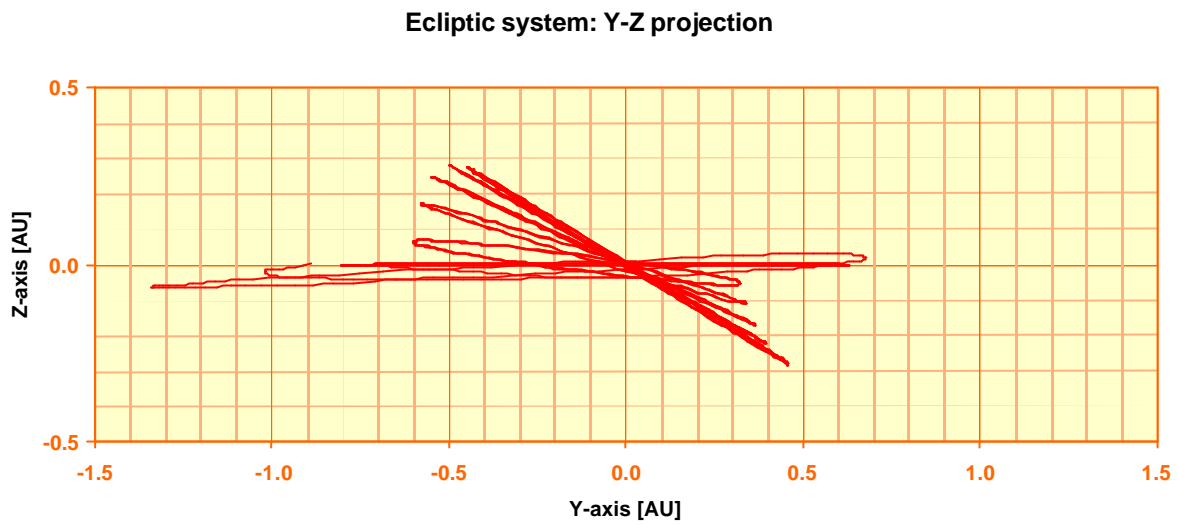


Figure 2-14. Ballistic transfer, 2015 launch: projection of the trajectory on the ecliptic system (y, z)-plane.

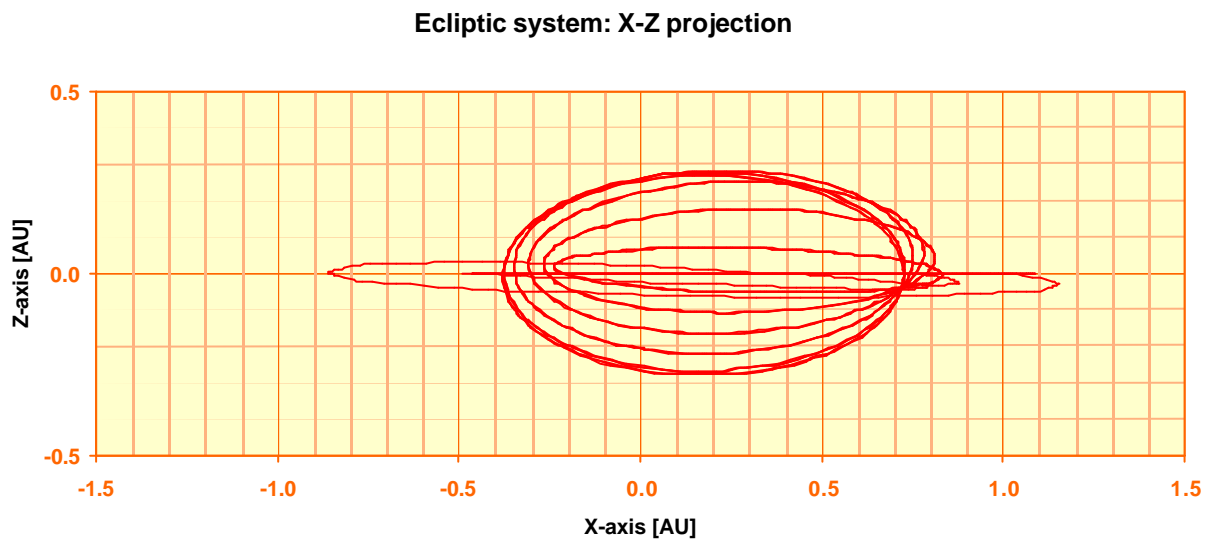


Figure 2-15. Ballistic transfer, 2015 launch: projection of the trajectory on the ecliptic system (x, z)-plane.

For each perihelion passage, Table 2-5 lists the distance to Sun centre in AU and solar radii, the spacecraft inertial orbit rotation rate (angular rate of the true anomaly) and rate relative to the rotating Sun in °/day in terms of the perihelion passage date and flight time.

Perihelion number	Date Perihelion	Flight time		Dist. to Sun		Rate [°/d]	
		Days	Years	[AU]	[SR]	inertial	/Sun
PER 1	2015-10-31	162	0.44	0.674	145	2.0	-12.2
PER 2	2016-12-29	587	1.61	0.460	99	3.8	-10.4
PER 3	2017-09-07	839	2.30	0.460	99	3.8	-10.4
PER 4	2018-05-15	1089	2.98	0.460	99	3.7	-10.4
PER 5	2018-11-17	1275	3.49	0.225	48	11.6	-2.6
PER 6	2019-04-16	1425	3.90	0.225	48	11.6	-2.6
PER 7	2019-09-12	1574	4.31	0.225	48	11.6	-2.6
PER 8	2020-02-13	1728	4.73	0.252	54	9.6	-4.5
PER 9	2020-07-11	1877	5.14	0.252	54	9.6	-4.5
PER 10	2020-12-08	2027	5.55	0.252	54	9.6	-4.5
PER 11	2021-05-12	2182	5.97	0.295	63	7.4	-6.7
PER 12	2021-10-09	2332	6.39	0.295	63	7.4	-6.7
PER 13	2022-03-08	2482	6.80	0.295	63	7.4	-6.7
PER 14	2022-08-14	2641	7.23	0.342	74	5.8	-8.4
PER 15	2023-01-11	2791	7.64	0.342	74	5.8	-8.4
PER 16	2023-06-09	2940	8.05	0.342	74	5.8	-8.4
PER 17	2023-11-19	3103	8.50	0.375	81	4.9	-9.2
PER 18	2024-04-17	3253	8.91	0.375	81	4.9	-9.2
PER 19	2024-09-13	3402	9.31	0.375	81	4.9	-9.2
PER 20	2025-02-14	3556	9.74	0.378	81	4.9	-9.3
PER 21	2025-07-14	3706	10.15	0.378	81	4.9	-9.3
PER 22	2025-12-11	3856	10.56	0.378	81	4.9	-9.3

Table 2-5. Distance to Sun centre in AU and solar radii, spacecraft inertial orbit rotation rate and rate relative to the rotating Sun in °/day in terms of the perihelion passage number, passage date and flight time.

The following set of diagrams (Figure 2-16 to Figure 2-20) show

6. The distance of the spacecraft from Earth, Venus and Sun function of flight time in days.
7. The angle Sun-Spacecraft-Earth and Sun-Earth-Spacecraft and the distance of the spacecraft to the Sun [AU] function of flight time in days.
8. The solar latitude function of flight time in days.
9. The solar latitude in terms of the distance of the spacecraft to the Sun [AU].
10. The solar radiation integrated doses function of flight time in days.

Distance Spacecraft-Earth, -Venus and -Sun

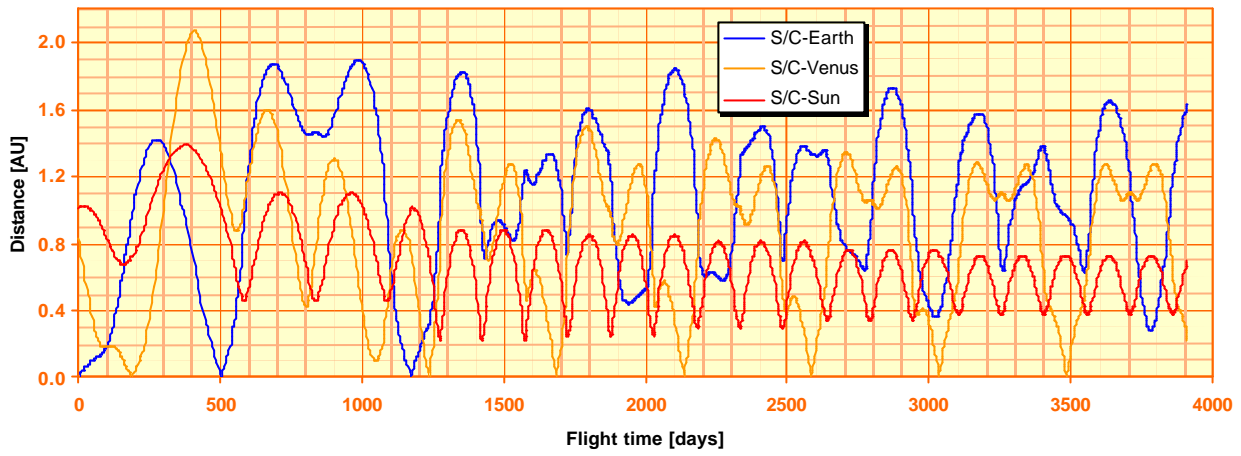


Figure 2-16. Ballistic transfer, 2015 launch: distance of the spacecraft from Earth, Venus and Sun function of flight day.

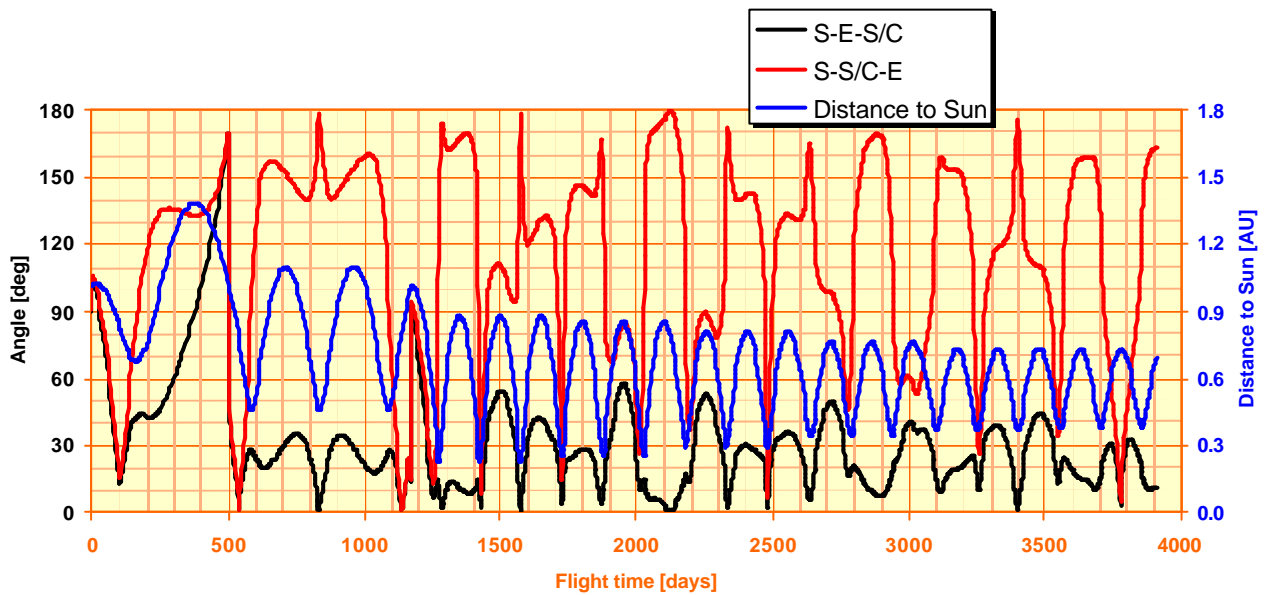


Figure 2-17. Ballistic transfer, 2015 launch: angle Sun-Spacecraft-Earth and Sun-Earth-Spacecraft and distance to Sun centre [AU] function of flight day.

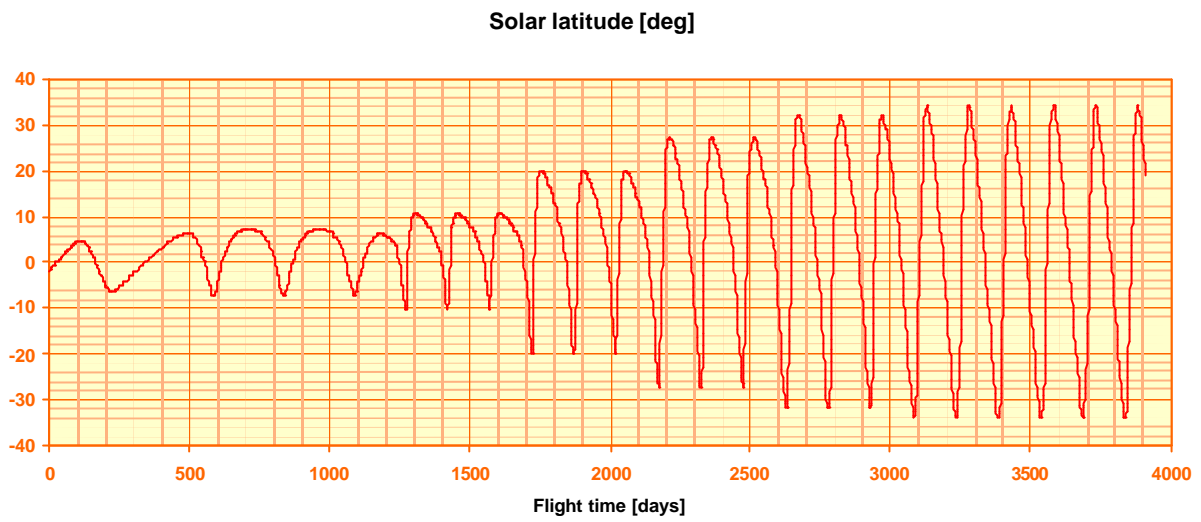


Figure 2-18. Ballistic transfer, 2015 launch: solar latitude function of flight day.

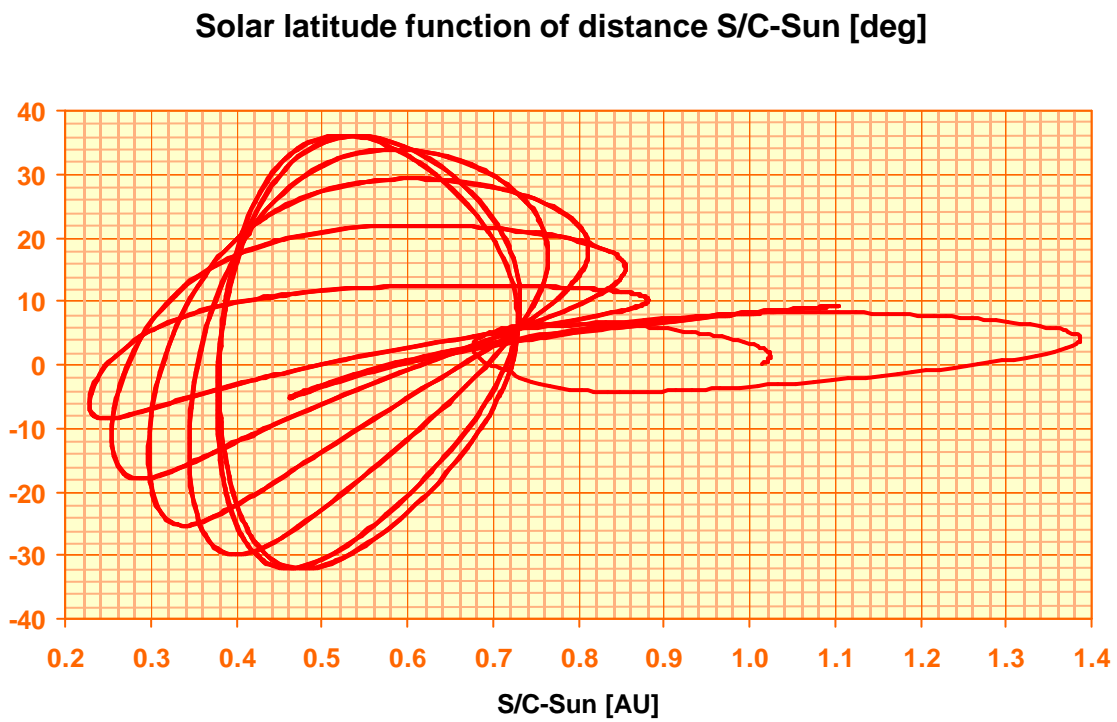


Figure 2-19. Ballistic transfer, 2015 launch: solar latitude function of distance Spacecraft-Sun.

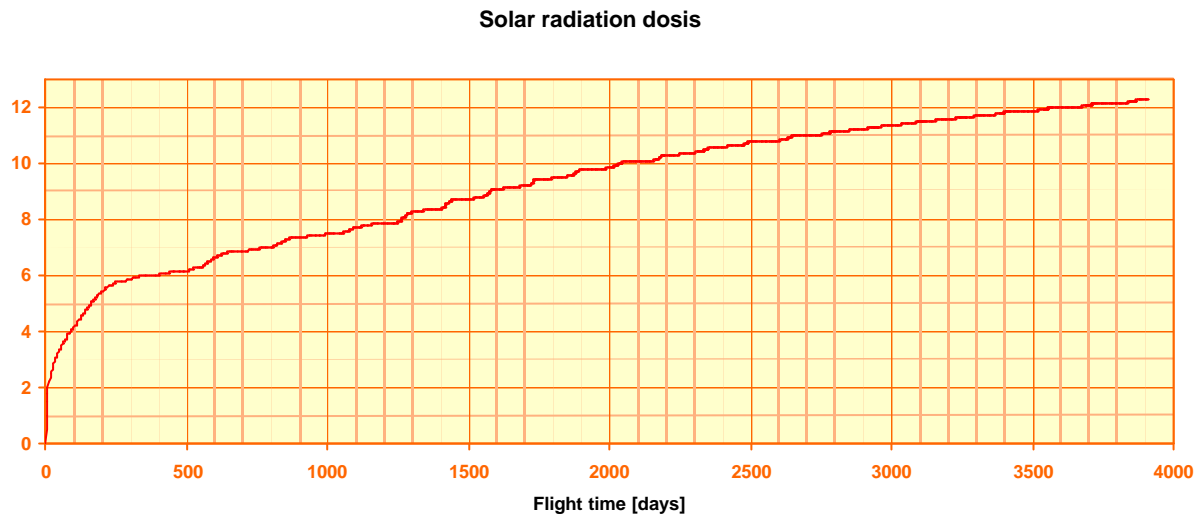


Figure 2-20. Ballistic transfer, 2015 launch: solar radiation integrated doses function of flight day.

Finally, coverage in hours/day from station New Norcia and Cebreros is shown respectively on Figure 2-21 and Figure 2-22 for 10° and 30° minimum elevation.

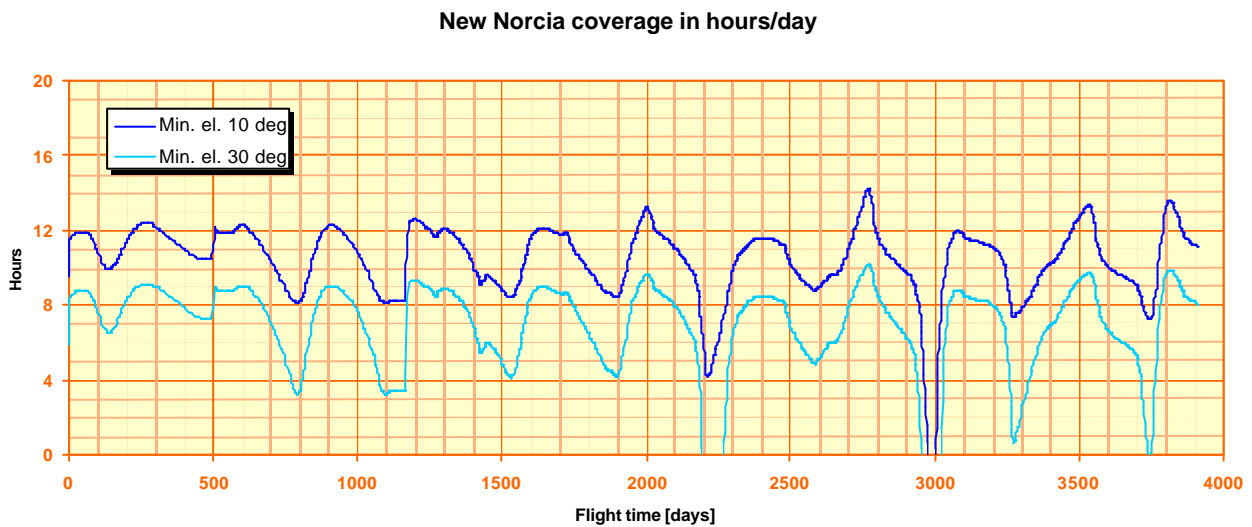


Figure 2-21. Ballistic transfer, 2015 launch: coverage in hours/day from New Norcia function of flight day.

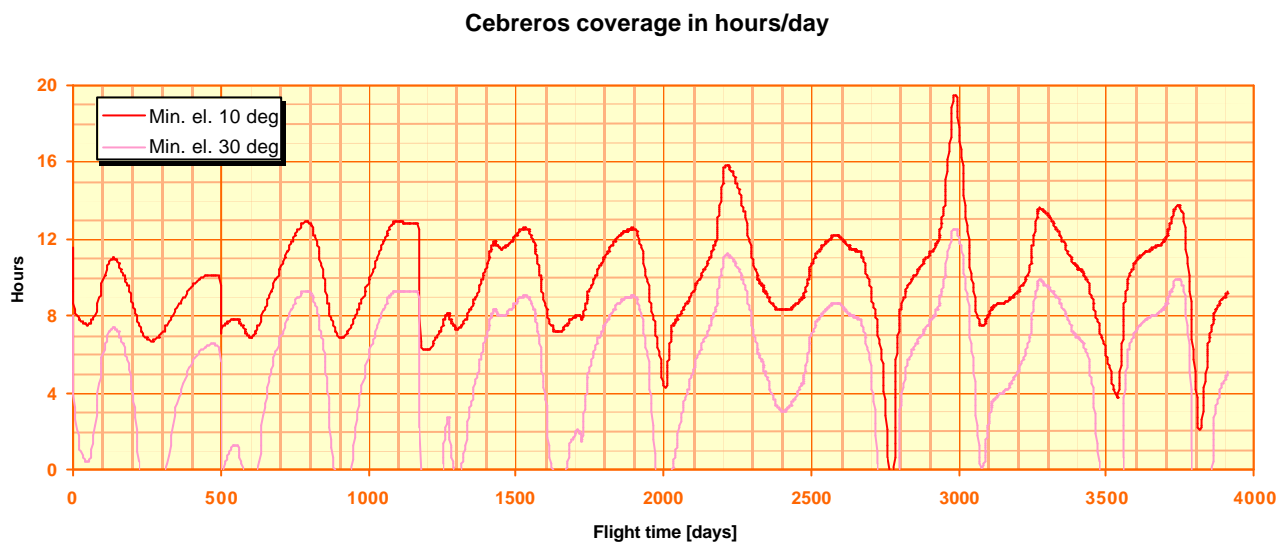


Figure 2-22. Ballistic transfer, 2015 launch: coverage in hours/day from Cebreros function of flight day.

2.5 2017 Launch

The mass budget table for a 2017 ballistic mission is shown in Table 2-1 columns headed 2017. Due to the absence of a sizable DSM and an escape velocity requirement slightly inferior to the 2015 launch, the mass budget is very favourable: spacecraft dry mass: 1172 kg.

The mission timeline for an optimum transfer in 2017 is shown in Table 2-6.

Date	Flight time		Event	Inclination [°]		Aphelion [AU]	Perihelion	
	Days	Years		Ecliptic	Sol. equ.		[AU]	[Sol. rad.]
2017-01-05	0	0	Launch	2.2	5.5	0.983	0.660	142
2017-04-17	102	0.28	GAM V1	2.0	7.0	1.477	0.720	155
2018-08-24	596	1.63	GAM E1	2.2	7.0	1.110	0.417	90
2020-08-23	1327	3.63	GAM E2	3.3	8.7	1.054	0.331	71
2021-02-08	1495	4.09	GAM V2	10.0	15.8	0.919	0.275	59
2022-12-14	2169	5.94	GAM V3	8.3	14.0	0.874	0.230	49
2024-03-08	2619	7.17	GAM V4	17.5	23.3	0.843	0.261	56
2024-07-31	2764	7.57	ENM	17.5	23.3	0.843	0.261	56
2025-05-31	3068	8.40	GAM V5	24.3	30.1	0.798	0.306	66
2026-08-23	3518	9.63	GAM V6	28.4	34.2	0.753	0.351	76
2026-10-30	3586	9.82	EXM	28.4	34.2	0.753	0.351	76
2027-11-16	3967	10.86	GAM V7	29.9	35.7	0.728	0.376	81
2028-12-30	4377	11.98	EOM	29.9	35.7	0.728	0.376	81

Table 2-6. Ballistic mission timeline for a launch in 2017.

Finding an optimum transfer for the 2017 launch was quite laborious and the transfer found is less favourable than for the 2013, 2015 and 2018 launches. In Table 2-7 a comparison between the 2015 and 2017 transfers in terms of duration between consecutive GAMs is shown.

	2015		2017		Difference
	Flight time	Duration	Flight time	Duration	
V1	188	317	102	494	177
E1	505	669	596	731	62
E2	1174	62	1327	168	106
V2	1236		1495		

Table 2-7. Timeline comparison between Venus GAM 1 and 2 for the 2015 and 2017 transfer. Flight times and duration between two consecutive GAMs are in days. Last column shows the increase in duration between the 2017 and 2015 case.

In spite of having a short transfer to Venus in 2017 (102 instead of 188 days), the trajectory arcs between subsequent GAMs are all longer so that the total transfer time is 259 days longer than for the other launch years. In addition, between GAM V1 and E1 the trajectory reaches a distance of 1.48 AU from the Sun (on flight day 316). For the 2015 transfer, the spacecraft does not exceed 1.38 AU (on flight day 377, 5 days after DSM).

The arrival geometry at Venus GAM 2 is not as favourable as for the other launch years and only a 4:3 resonant orbit with Venus with a period of 169 days and a perihelion radius of 0.28 AU can be achieved. This adds another Venus orbit period (224.7 days) to the mission so that the ENM occurs 16 months later than for the other launch years. The ENM for the 2018 launch (Section 2.6) will occur only six weeks later than ENM for the 2017 launch.

First PMSL after Venus GAM 4 occurs on 2024-05-27 and ENM is defined two months later, on 2024-07-31. EXM is defined on 2026-10-30, about a week after first PMSL following GAM 6 on 2026-10-24. Finally, EOM is defined on 2028-12-30, after three PMSLs following GAM 7.

Figure 2-23 shows the projection of the trajectory on the ecliptic plane and symbols represent DSMs and GAMs until Venus GAM 2. Figure 2-24 and Figure 2-25 show the projection of the trajectory on the ecliptic system (y, z)-plane and (x, z)-plane respectively.

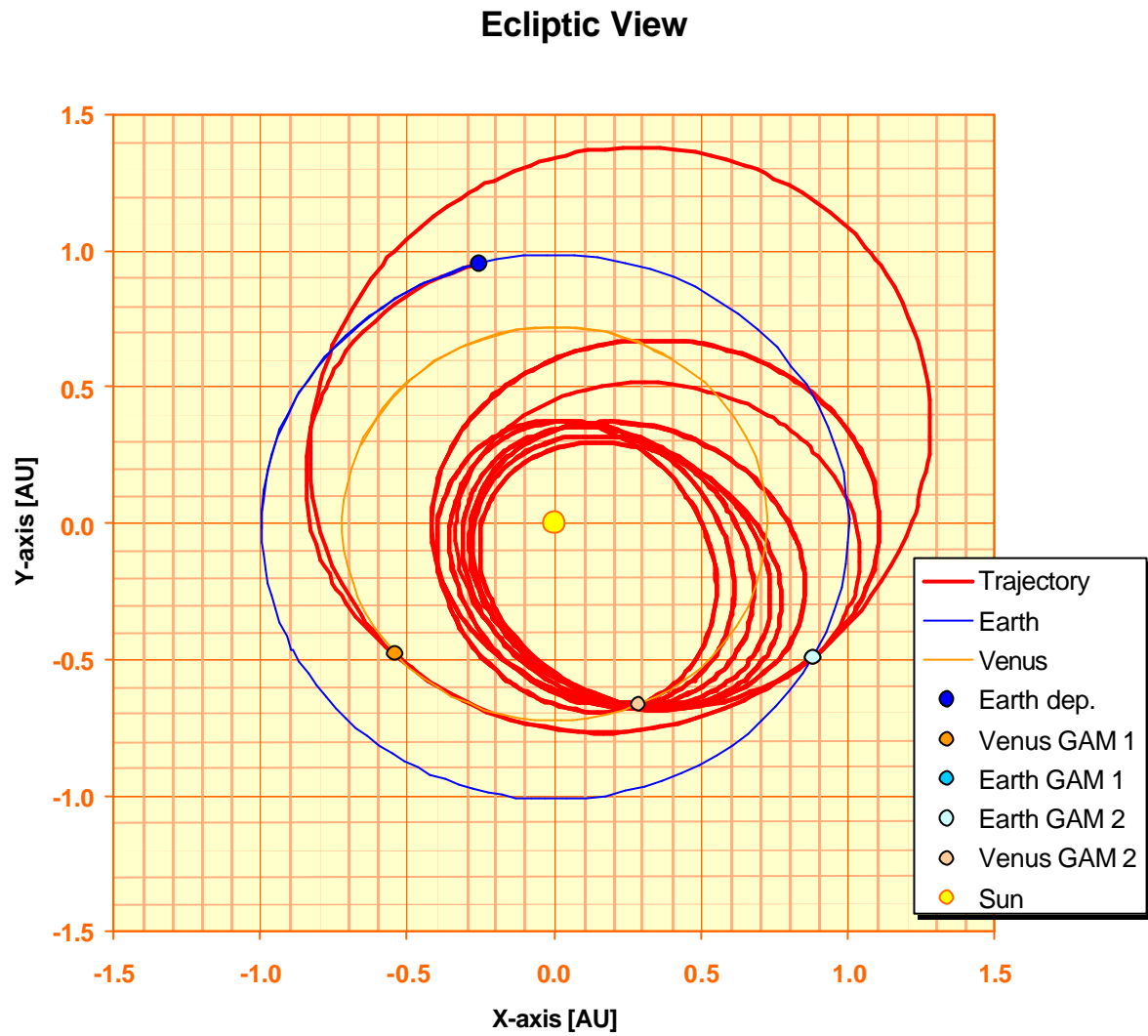


Figure 2-23. Ballistic transfer, 2017 launch: ecliptic view of the trajectory, GAMs until Venus GAM 2 and DSMs.

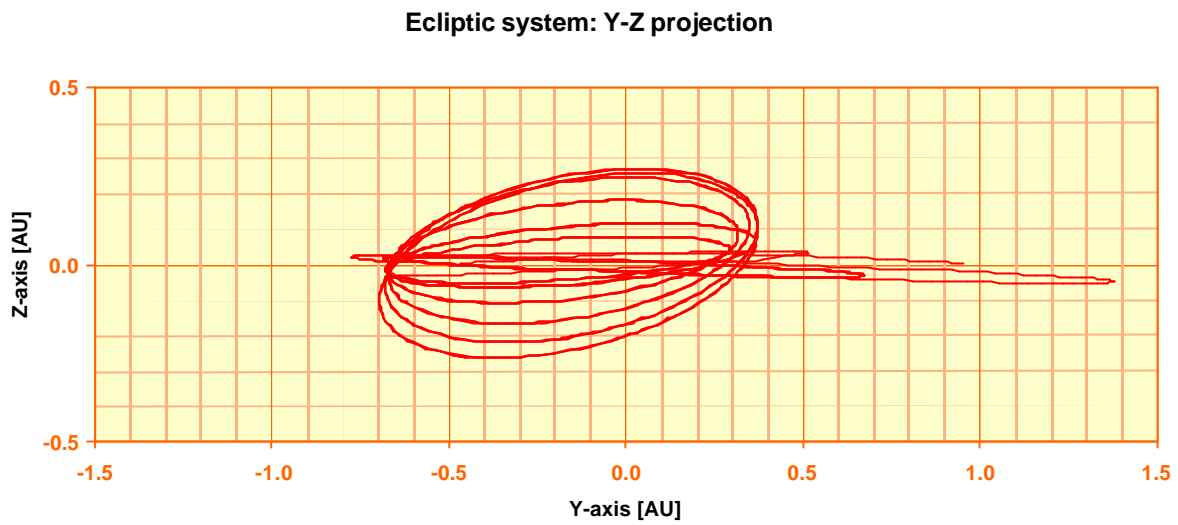


Figure 2-24. Ballistic transfer, 2017 launch: projection of the trajectory on the ecliptic system (y, z)-plane.

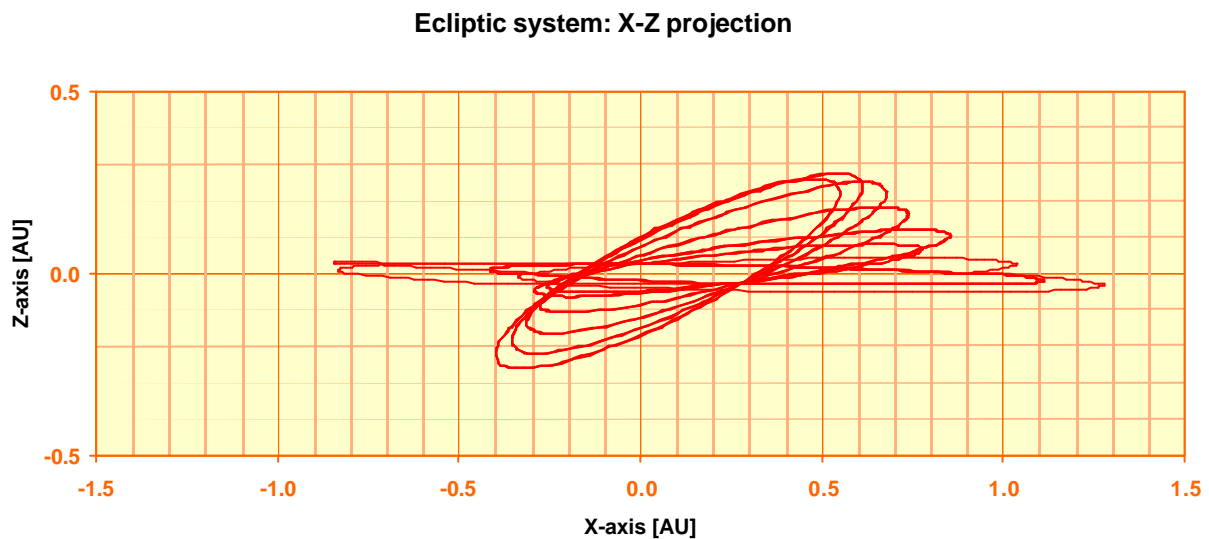


Figure 2-25. Ballistic transfer, 2017 launch: projection of the trajectory on the ecliptic system (x, z)-plane.

For each perihelion passage, Table 2-8 lists the distance to Sun centre in AU and solar radii, the spacecraft inertial orbit rotation rate and rate relative to the rotating Sun in $^{\circ}/\text{day}$ in terms of the perihelion passage date and flight time.

Perihelion number	Date Perihelion	Flight time		Dist. to Sun		Rate [°/d]	
		Days	Years	[AU]	[SR]	inertial	/Sun
PER 1	2017-04-23	108	0.30	0.720	155	1.9	-12.3
PER 2	2018-06-18	530	1.45	0.720	155	1.9	-12.3
PER 3	2019-02-05	761	2.08	0.417	90	4.4	-9.8
PER 4	2019-10-06	1004	2.75	0.417	90	4.4	-9.8
PER 5	2020-06-05	1247	3.41	0.417	90	4.4	-9.8
PER 6	2020-12-31	1457	3.99	0.331	71	6.4	-7.8
PER 7	2021-06-16	1623	4.44	0.275	59	8.4	-5.7
PER 8	2021-12-02	1792	4.91	0.275	59	8.5	-5.7
PER 9	2022-05-19	1960	5.37	0.275	59	8.4	-5.7
PER 10	2022-11-04	2129	5.83	0.275	59	8.5	-5.7
PER 11	2023-04-03	2279	6.24	0.230	49	11.2	-3.0
PER 12	2023-08-31	2429	6.65	0.230	49	11.2	-3.0
PER 13	2024-01-28	2579	7.06	0.230	49	11.2	-3.0
PER 14	2024-06-23	2726	7.46	0.261	56	9.1	-5.1
PER 15	2024-11-20	2876	7.87	0.261	56	9.1	-5.1
PER 16	2025-04-19	3026	8.28	0.261	56	9.1	-5.1
PER 17	2025-09-09	3169	8.68	0.306	66	7.0	-7.2
PER 18	2026-02-06	3319	9.09	0.306	66	7.0	-7.2
PER 19	2026-07-05	3468	9.50	0.306	66	7.0	-7.2
PER 20	2026-11-22	3609	9.88	0.351	76	5.5	-8.7
PER 21	2027-04-21	3759	10.29	0.351	76	5.5	-8.7
PER 22	2027-09-18	3909	10.70	0.351	76	5.5	-8.7
PER 23	2028-02-01	4044	11.07	0.376	81	4.9	-9.3
PER 24	2028-06-30	4194	11.48	0.376	81	4.9	-9.3
PER 25	2028-11-27	4344	11.89	0.376	81	4.9	-9.3

Table 2-8. Distance to Sun centre in AU and solar radii, spacecraft inertial orbit rotation rate and rate relative to the rotating Sun in °/day in terms of the perihelion passage number, passage date and flight time.

The following set of diagrams (Figure 2-26 to Figure 2-30) show

11. The distance of the spacecraft from Earth, Venus and Sun function of flight time in days.
12. The angle Sun-Spacecraft-Earth and Sun-Earth-Spacecraft and the distance of the spacecraft to the Sun [AU] function of flight time in days.
13. The solar latitude function of flight time in days.
14. The solar latitude in terms of the distance of the spacecraft to the Sun [AU].
15. The solar radiation integrated doses function of flight time in days.

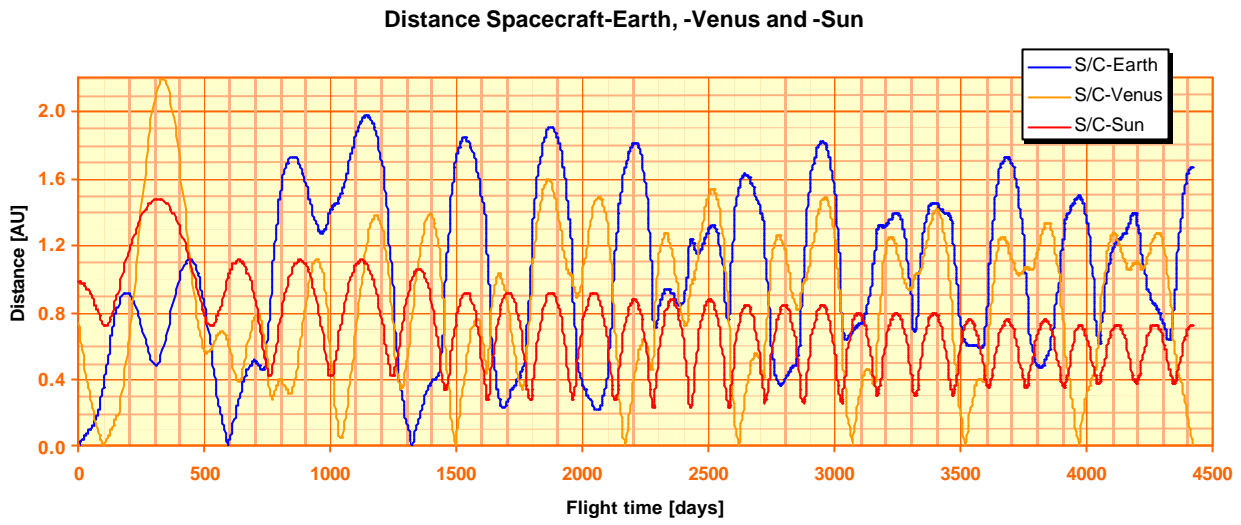


Figure 2-26. Ballistic transfer, 2017 launch: distance of the spacecraft from Earth, Venus and Sun function of flight day.

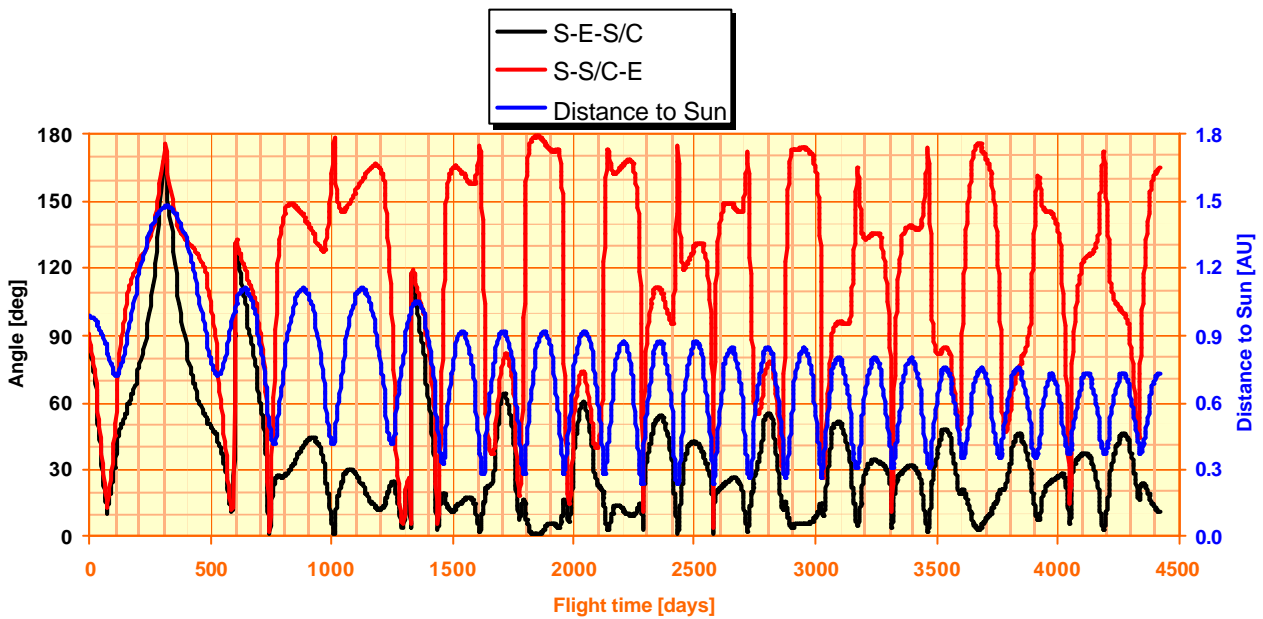


Figure 2-27. Ballistic transfer, 2017 launch: angle Sun-Spacecraft-Earth and Sun-Earth-Spacecraft and distance to Sun centre [AU] function of flight day.

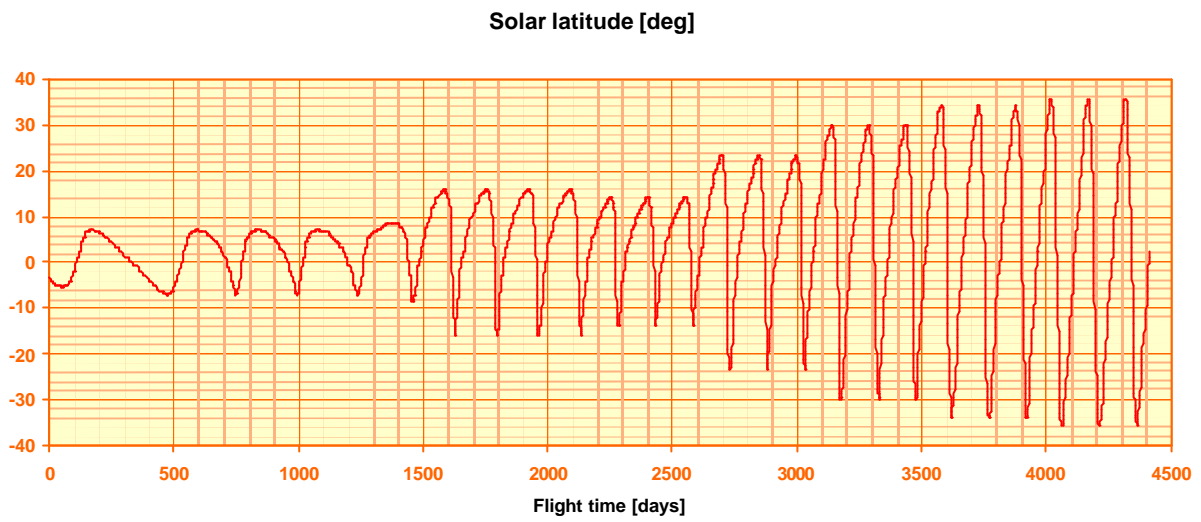


Figure 2-28. Ballistic transfer, 2017 launch: solar latitude function of flight day.

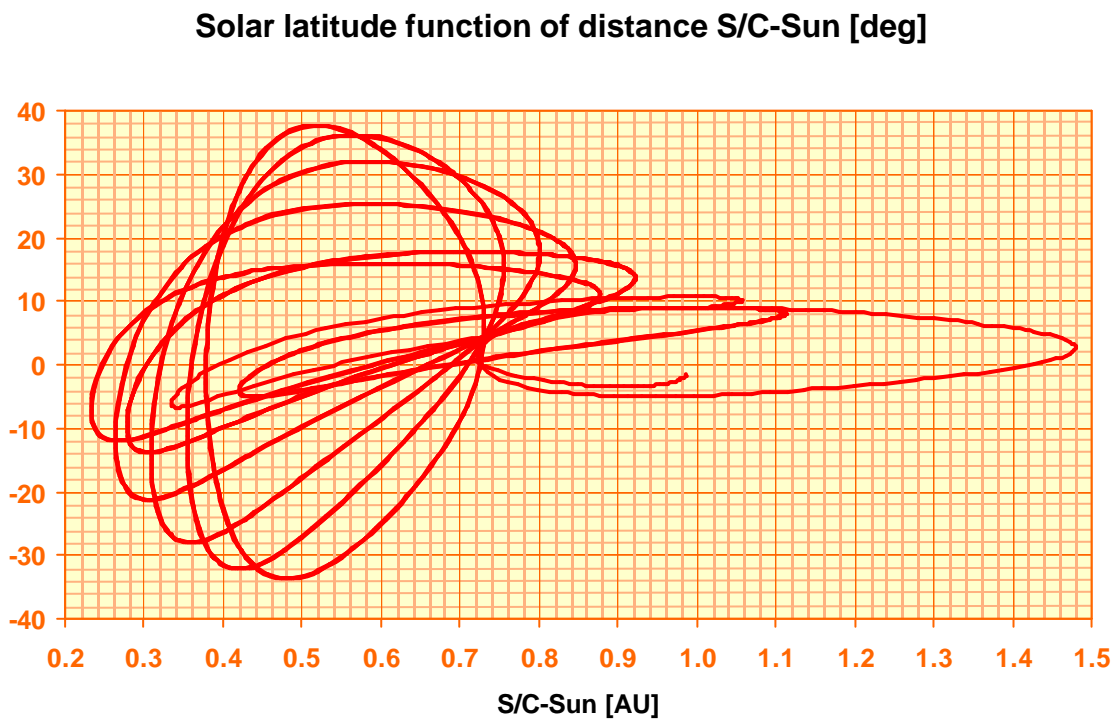


Figure 2-29. Ballistic transfer, 2017 launch: solar latitude function of distance Spacecraft-Sun.

Solar radiation dosis

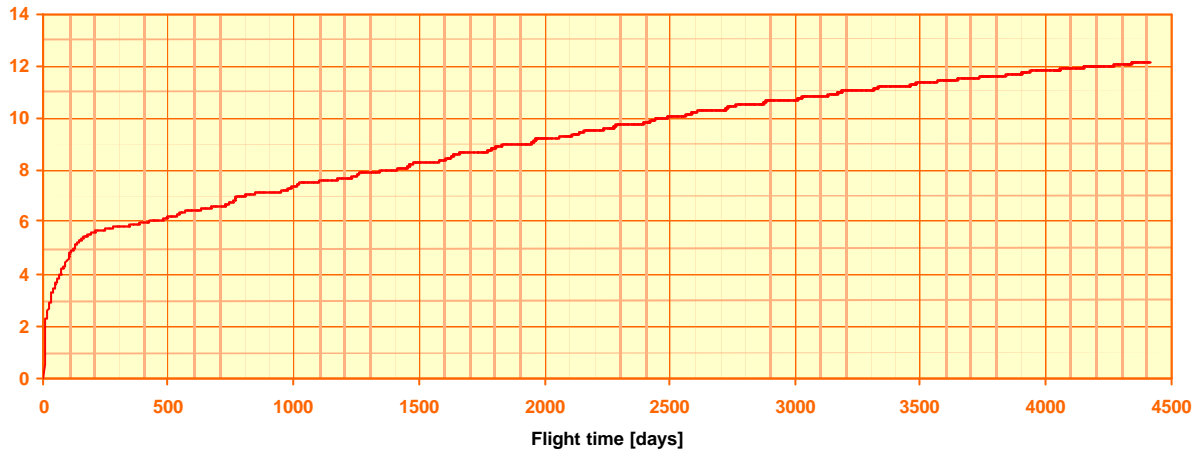


Figure 2-30. Ballistic transfer, 2017 launch: solar radiation integrated doses function of flight day.

Finally, coverage in hours/day from station New Norcia and Cebreros is shown respectively on Figure 2-31 and Figure 2-32 for 10° and 30° minimum elevation.

New Norcia coverage in hours/day

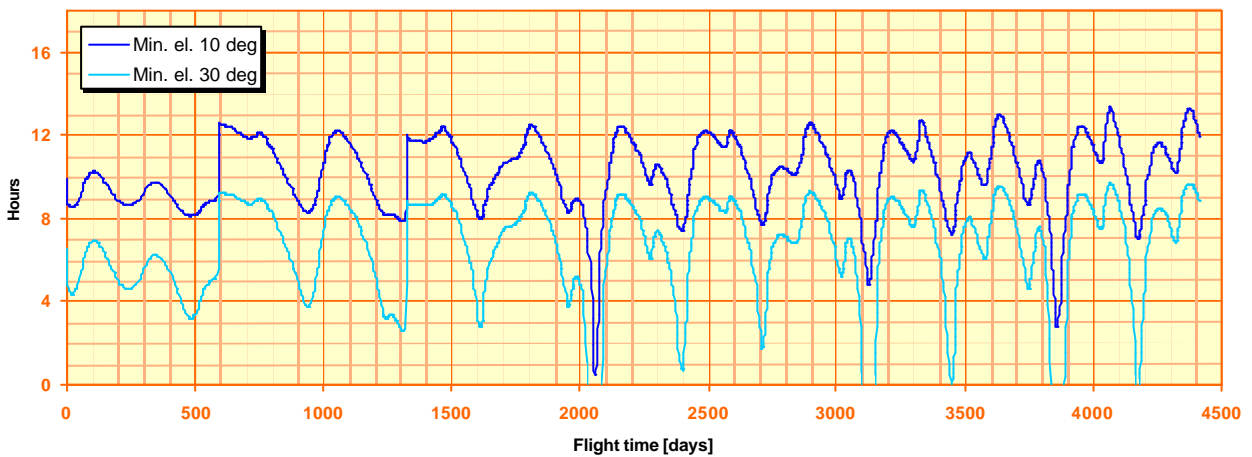


Figure 2-31. Ballistic transfer, 2017 launch: coverage in hours/day from New Norcia function of flight day.

Cebberos coverage in hours/day

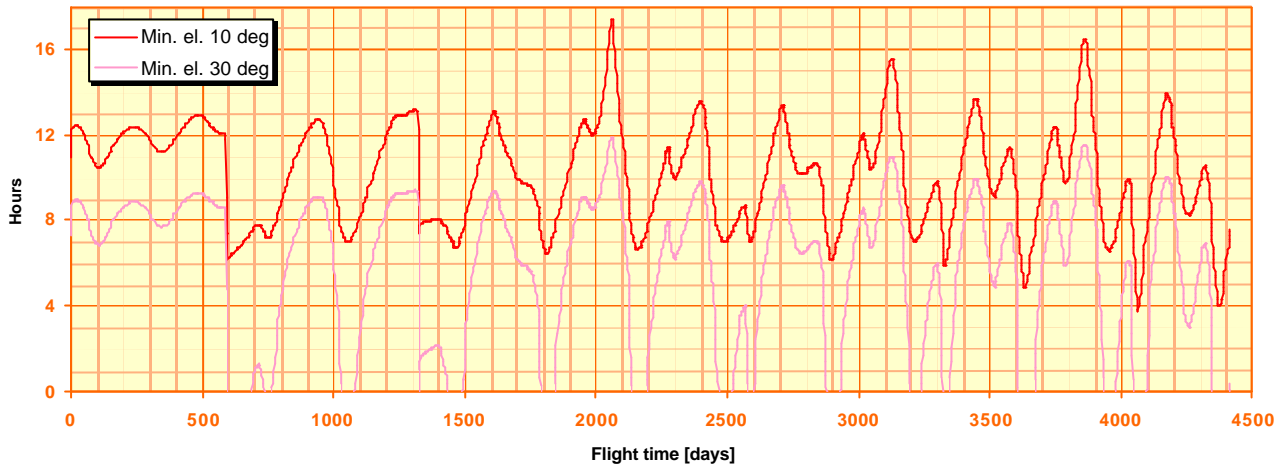


Figure 2-32. Ballistic transfer, 2017 launch: coverage in hours/day from Cebberos function of flight day.

2.6 2018 Launch

The mass budget table for a 2018 ballistic mission is shown in Table 2-1 columns headed 2018.

The mission timeline up to EXM for an optimum transfer in 2018 is shown in Table 2-9. In addition to flight time, inclination relative to the ecliptic plane and the solar equator, aphelion and perihelion radius in AU are listed. This timeline is very similar to the 2013 and 2015 launch opportunity.

Date	Flight time		Event	Inclination [°]		Aphelion [AU]	Perihelion	
	Days	Years		Ecliptic	Sol. equ.		[AU]	[Sol. rad.]
2018-08-05	0	0	Launch	4.1	6.1	1.015	0.694	149
2018-11-21	108	0.30	DSM 1	4.1	5.9	1.003	0.691	148
2019-01-27	175	0.48	GAM V1	3.3	3.9	1.366	0.720	155
2019-12-12	494	1.35	GAM E1	0.0	7.3	1.085	0.475	102
2021-10-10	1162	3.18	GAM E2	0.1	7.3	1.006	0.322	69
2021-12-19	1232	3.37	GAM V2	3.5	3.8	0.873	0.231	50
2023-03-13	1682	4.60	GAM V3	7.5	14.7	0.861	0.243	52
2024-06-05	2131	5.83	GAM V4	16.6	23.9	0.828	0.276	59
2024-09-09	2227	6.10	ENM	16.6	23.9	0.828	0.276	59
2025-08-28	2580	7.06	GAM V5	23.1	30.3	0.781	0.323	70
2026-11-20	3030	8.30	GAM V6	26.7	34.0	0.736	0.368	79
2027-03-16	3146	8.61	EXM	26.7	34.0	0.736	0.368	79

Table 2-9. Ballistic mission timeline for a launch in 2018.

First PMSL after Venus GAM 4 occurs on 2024-08-14 and ENM is defined about four weeks later, on 2024-09-09. EXM is defined on 2027-03-16, a month after first PMSL following GAM 6 on

2027-02-18. Finally, EOM (not listed in Table 2-9) is defined on 2029-04-14, after three PMSLs following GAM 7.

2.7 Launch Window

The launch window is a period in time when launch leads to a trajectory satisfying the mission requirements. In particular the mass budget has to be satisfied. To cope with this condition a so-called launch window margin is included in the mass budget. This margin is composed of two components: a launcher injection velocity and a DSM DV margin.

Following an earlier launch window investigation based on a ballistic mission in 2013 (Ref. 1), it was proposed for a 3-week launch window to take a margin of 130 m/s on the escape velocity and 58 m/s on the DSM DV .

Such an investigation was repeated for a 2015 launch. Five launch dates at one week interval around the optimum date were selected and the corresponding trajectory was optimised. The result in terms of escape velocity and DSM DV is shown on Figure 2-33.

Figure 2-33 confirms that, for a selected 3-week optimum interval between May 8 and May 29, the launch window penalty and the total DSM DV are well within the margins adopted.

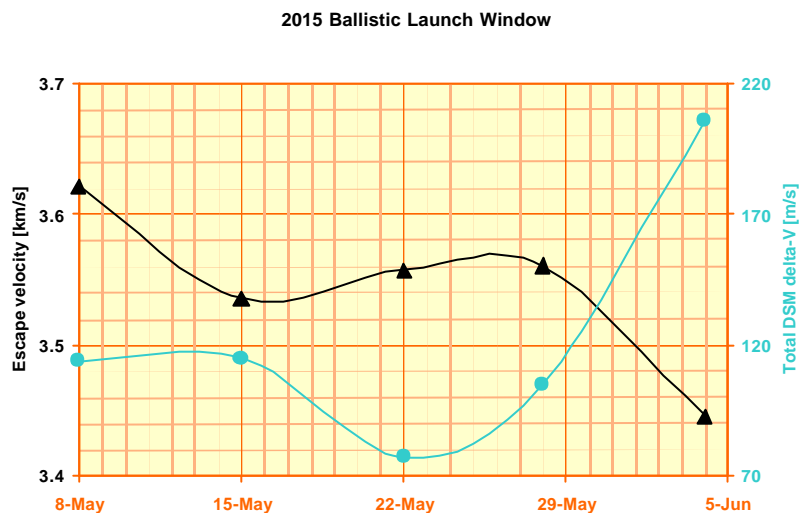


Figure 2-33. Variation in escape velocity and total DSM DV for optimum launches between May 8 and June 4, 2015.

PAGE INTENTIONALLY LEFT BLANK

3. INCLINATION INCREASE

3.1 Procedure for Inclination Increase

A main scientific requirement for the Solar Orbiter mission is to reach an orbit with a high inclination relative to the solar equator.

During transfer phase aiming at reducing the perihelion radius, GAMs with Venus and Earth are performed constraining the trajectory to be close to the ecliptic plane. This precludes major change in orbit inclination. When the Low Solar Orbit (LSO) with the desired perihelion radius is reached, a procedure for raising the inclination can be started.

Inclination changes are very demanding in DV and it would be very costly to entrust them to the orbit propulsion unit. A planetary GAM on the other way provides an efficient way to change the direction of the orbit velocity vector, therefore it can be used for inclination changes. As only a small change can be achieved in one GAM, a series of successive GAMs has to be performed. This can be achieved only by having an orbit, which period is in resonance with the period of the planet used for the GAMs.

Venus and Mercury are the only planets entering into consideration for repeated GAMs on a LSO. Venus having a mass 21 times larger than Mercury, is the best choice. A resonant 1:1 orbit with Venus would allow passing through perihelion once every Venus year (224.7 years). Ideal would be a 2:1 orbit of 112-day period. However the corresponding perihelion radius would be of the order of 0.15 AU. As the thermal stress on the satellite when passing to such a short distance to the Sun is too high, choice is left to intermediate orbits. The 3:2 resonance seems to be the best compromise. Characteristics of the corresponding orbit are:

- Semi-major axis: 82580000 km = 0.552 AU
- Period: 149.8 days

Efficiency of the Venus GAM depends on the magnitude and direction of the relative (hyperbolic) arrival velocity and the date of the encounter. Higher the hyperbolic velocity and closer the position of Venus at encounter relative to the node with the solar equator, higher will be the inclination gain. However, a high relative velocity will cause the perihelion radius to be low. This is illustrated on Figure 3-1 in the ideal case of an arrival velocity vector in the plane of Venus orbit.

Inclination increase through GAMs is maximal when the orbit plane of the spacecraft is close to the plane of Venus orbit. When inclination is raised, GAMs become less efficient until a maximum inclination is reached. When performing the last Venus GAM leading to the maximum inclination it is also possible to aim to a slightly smaller inclination and use major part of the

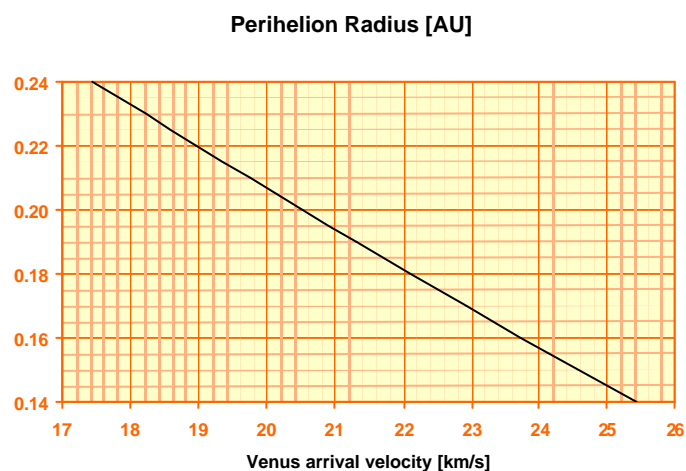


Figure 3-1. Relation between perihelion radius and planar Venus hyperbolic arrival velocity for a 3:2 resonant orbit with Venus.

swing-by energy to reduce the perihelion radius. This was proposed in Ref. 1 where, at Venus GAM 6, the inclination was raised from 34.9° to 35.0° only while the perihelion radius was decreased from 0.357 to 0.248 AU.

To prevent a possible future crash on Venus it is recommended to aim toward a non-resonant orbit during the last Venus GAM. This has the additional advantage to offer more flexibility in the selection of orbit elements for the final orbit, such as a low perihelion radius.

3.2 Maximal Inclination Raise and Propellant Usage

The maximum inclination relative to the solar equator that can be achieved depends to a great deal on the magnitude of the Venus GAM 2 arrival velocity and the maximum reachable inclination is an almost linear function of the arrival velocity (Figure 3-2).

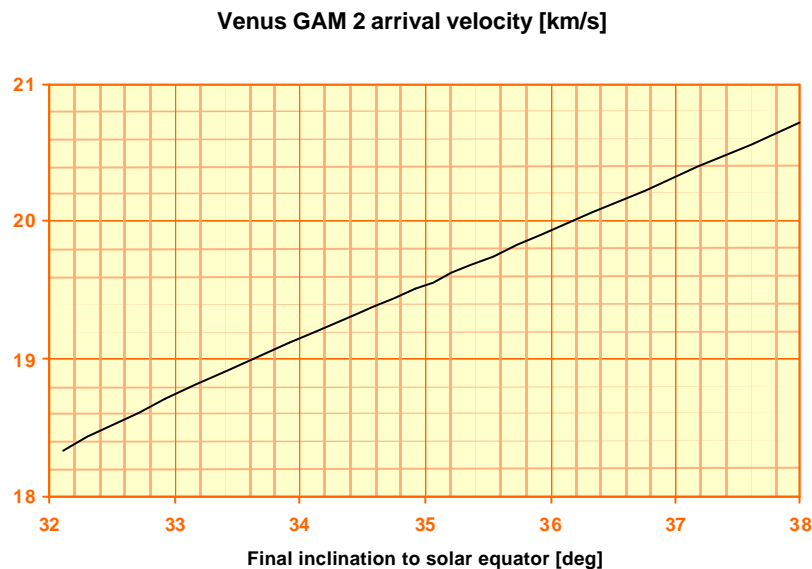


Figure 3-2. Arrival hyperbolic velocity at Venus GAM 2 in terms of reachable final inclination with respect to solar equator for the 2013 ballistic mission.

For targeting a new arrival velocity, the transfer trajectory has to be re-optimised and results in a new total DV . This total DV will be higher if the arrival velocity is higher and so the propellant usage.

To estimate such a propellant usage, for the case of a 2013 launch optimal transfer trajectories were calculated for a set of target Venus GAM 2 arrival velocities and corresponding maximum inclination was computed. Resulting propellant mass changes are shown on Figure 3-3 in the form of Δ -propellant mass given relative to the baseline case.

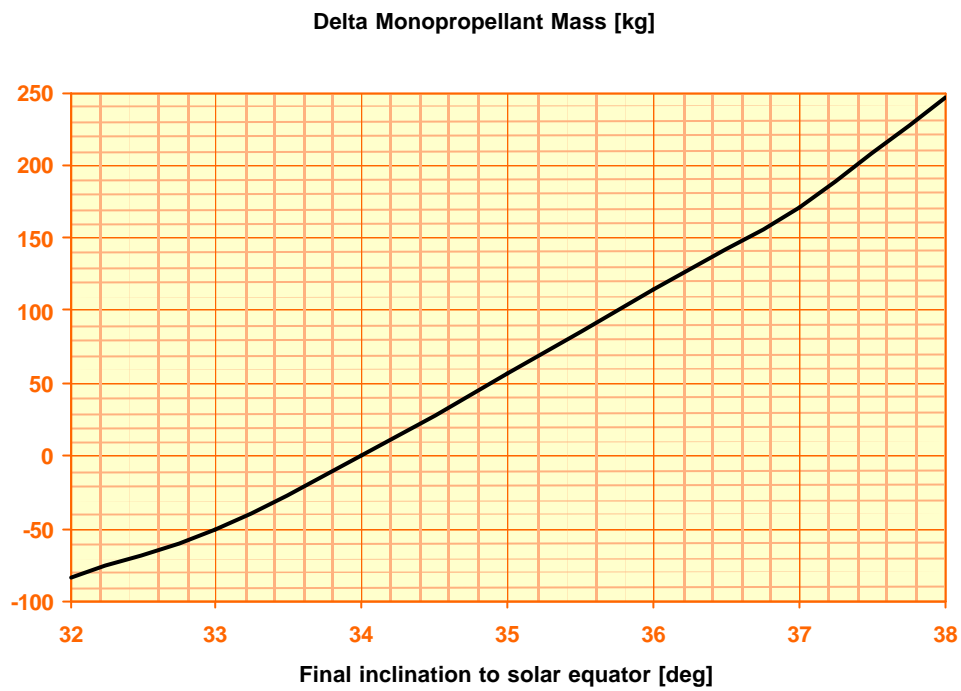


Figure 3-3. Δ -monopropellant mass in terms of the reachable final inclination relative to the solar equator for a CP mission.

Figure 3-2 and Figure 3-3 are to be considered as indicative as they depend on the transfer trajectory, therefore on the launch year, on launcher performance and propulsion unit specific impulse.

PAGE INTENTIONALLY LEFT BLANK

4. NAVIGATION

4.1 Introduction

This chapter intends to analyse the navigation performances when using the AOCS during the Science phase of the mission.

The manoeuvres used in the guidance process are applied with the help of a monopropellant propulsion system with a specific impulse of 220 s. The number and implementation date of the manoeuvres have been selected based on the experience of previous similar studies.

A covariance analysis is used to estimate position and velocity of the spacecraft. Both the knowledge and the dispersion covariance matrixes are propagated and updated along the reference trajectory.

Only two arcs were analysed (Table 4-1):

1. A 100-day long arc preceding GAM Venus 2.
2. The arc between Venus GAM 2 and 3, considered being representative for the inclination rise phase.

Arc	Begin			End			Duration (days)
	Reference	Calendar	MJD2000	Ref.	Calendar	MJD2000	
1	GAM V2-100	2015-05-02	5600.5	GAM V2	2015/8/10	5700.5	100
2	GAM V2+10	2015-08-20	5710.5	GAM V3	2016/11/1	6149.5	439

Table 4-1. Description of the arcs analysed in this working paper. GAM V2: 2nd Venus swing-by. GAM V3: 3rd Venus swing-by.

4.2 Models and Assumptions

4.2.1 Spacecraft

For this navigation analysis the following characteristics of the spacecraft was taken:

- Reflectivity coefficient: 1.0
- Ratio area-to-mass: $S/m = 0.02 \text{ m}^2/\text{kg}$

4.2.2 Measurements

For the measurements the following is assumed:

- Two-way range and Doppler data are acquired from two ground stations: New Norcia and Cebros.
- The minimum elevation is set to 5° for each ground station.

- During the 10-day interval prior to a Trajectory Correction Manoeuvre (TCM), the range data are sampled at a rate of 1 measurement every hour, and the Doppler data at a rate of 1 measurement every 10 minutes. Otherwise, the range and Doppler data are sampled at a rate of 1 measurement every day.
- To account for data noise, a 1σ random uncertainty of 10 m is added to the range measurement. For the Doppler measurement, the 1σ random uncertainty is assumed to be 0.3 mm/s.

4.2.3 Covariance Analysis

A batch-sequential Square Root Information Filter has been used to process the measurements, with a batch size of 1 day. The following is assumed:

- Initial dispersion 100-day prior to GAM V2:
 - Position (1σ): 200 km in each coordinate
 - Velocity (1σ): 2 m/s in each coordinate
- The initial spacecraft knowledge uncertainties are large enough to leave it essentially unconstrained:
 - Position (1σ): 200 km in each coordinate
 - Velocity (1σ): 2 m/s in each coordinate
- The initial knowledge and dispersion for the following Venus GAMs are taken at the exit of Venus sphere of influence. This process is repeated until the last Venus GAM.
- The biases on the ground stations location (X and Y axis are parallel to Earth equator) are accounted for as considered parameters:
 - X -coordinate: 1 m
 - Y -coordinate: 1 m
 - Z -coordinate: 3 m
- A 5 m bias is included in the range measurement as a consider parameter, in order to represent ranging system calibration errors.
- The solar radiation pressure uncertainty is modelled as a bias for GAM V2. Its value is taken equal to 0.5 % of the force coefficient $C_r S/m$, i.e. $0.00011 \text{ m}^2/\text{kg}$.
- All other uncertainty sources (e.g. non-gravitational accelerations, Venus ephemeris, etc) are supposed to be negligible in this analysis.

4.2.4 Guidance Algorithm

A fixed-time guidance law was used to compute the trim manoeuvres required to correct the trajectory before the swing-bys. The following is assumed:

- Three TCMs to be performed prior to GAM V2. The simulation starts 100 days before Venus encounter. The first TCM is applied 90 days before encounter. The second TCM is applied 25 days before while the third TCM is implemented 3 days before Venus encounter.

- For each following Venus GAM, the strategy is different due to the 3:2 resonant orbit of the spacecraft w.r.t. Venus:
 - A first TCM is applied 10 days after the previous Venus GAM
 - A TCM is applied each time the spacecraft completes one revolution. This corresponds to 2 TCMs
 - For the last revolution, one TCM is applied 15 days before planet encounter.

This leads to 4 TCMs between two successive Venus GAMs.

- The errors in the execution of the TCMs are assumed to be random noise. The 1σ uncertainty is:
 - Modulus: 1 %
 - Direction: 0.5°

4.3 Simulation Results

The estimates of the trim manoeuvres required to correct the trajectory deviations before a Venus gravity assist are presented in this section. The mean, the 95th percentile, the 99th percentile and the maximum value are given for each one of the TCMs. The percentiles are computed by means of a Monte Carlo analysis.

In order to characterize the delivery errors, the 1σ dispersion covariance matrix is mapped from every manoeuvre to the final time, i.e. the pericentre of the planetary hyperbola, and projected on the target plane. This plane is perpendicular to the spacecraft velocity vector at the pericentre and contains the target body centre of mass. The projection is an ellipse with semi-major axis SMAA and semi-minor axis SMIA. The Linear Time of Flight (LTF) is given along the normal to this plane, i.e. the spacecraft velocity. The radial value is the error in the altitude of the pericentre. The angle q is measured between the x -axis and the ellipse semi-major axis direction.

The x -direction is defined as the intersection of the projection plane and the Mean Earth Equator 2000. The z -direction is along the spacecraft velocity vector. The y -direction completes the right-handed frame.

4.3.1 Navigation Before the Second Venus Swing-by

Table 4-2 summarises the estimates of the correction manoeuvres.

Correction manoeuvre	Day	Mean (m/s)	Δv (95%) (m/s)	Δv (99%) (m/s)	Max (m/s)
TCM1	GAM V2 - 90	3.34	6.01	7.33	10.27
TCM2	GAM V2 - 20	0.55	1.10	1.36	2.02
TCM3	GAM V2 - 3	0.05	0.10	0.12	0.18

Table 4-2. Trajectory correction manoeuvres statistics before the second Venus encounter (GAM V2).

It appears that the propellant budget is a bit more than 10 m/s. It is clear that the main contribution comes from the first TCM. The remaining corrections are a refinement of the targeting.

Table 4-3 gives an overview of the achievable precision in the target plane. The size of the dispersion ellipse is reduced to an acceptable level after TCM2: the radial uncertainty is 9.6 km. However the last TCM does not improve the results. Indeed it only reduces the LTF that was already acceptable. Therefore it is recommended to apply only two TCMs.

Correction manoeuvre	Day	SMAA (km)	SMIA (km)	q (deg)	LTF (s)	Radial (km)
(Initial)	GAM V2 - 100	38860.8	8475.3	-4.9	806.8	31624.3
TCM1	GAM V2 - 90	706.5	556.6	-84.6	17.7	587.8
TCM2	GAM V2 - 20	9.6	5.4	33.1	0.6	9.6
TCM3	GAM V2 - 3	19.6	1.9	78.2	0.1	13.4

Table 4-3. Evolution of the 1σ dispersion covariance matrix at pericentre projected on the target plane (GAM V2).

The inefficiency of the last TCM is a consequence of a poor knowledge of the state vector as plotted in Figure 4-1 and Figure 4-2.

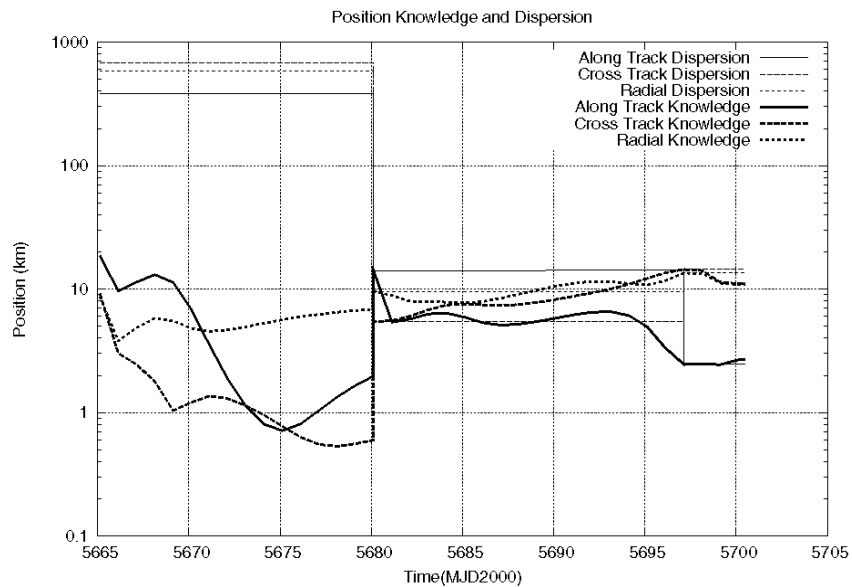


Figure 4-1. Evolution of the 1σ position knowledge (thick lines) and dispersion (thin lines) mapped to the pericentre (GAM V2).

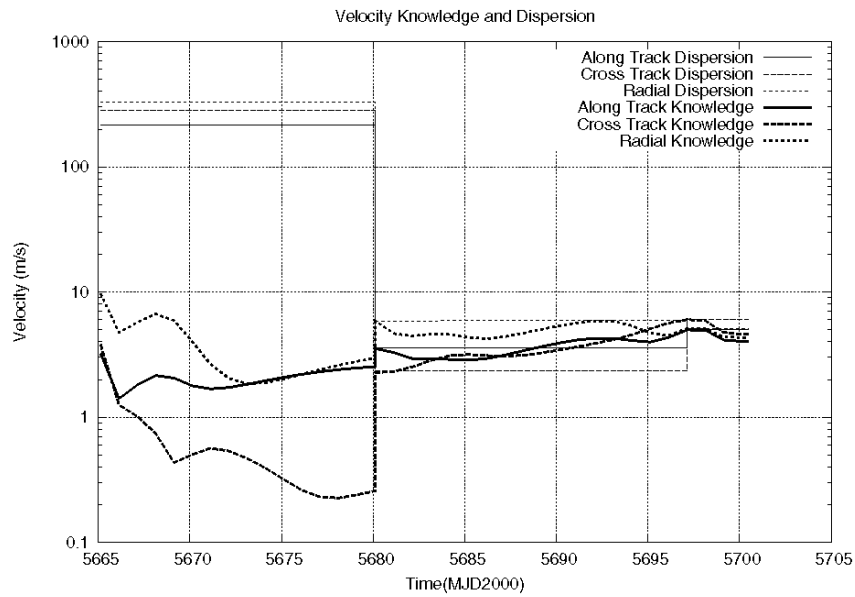


Figure 4-2. Evolution of the 1σ velocity knowledge (thick lines) and dispersion (thin lines) mapped to the pericentre (GAM V2).

Errors ellipses are given in Figure 4-3, along with the pericentre vector. Their projection along the radial direction yields the error in the swing-by altitude, that is the most critical component of the error. Before the second TCM (solid line on the left figure) it is obvious that the precision is not sufficient since the ellipse crosses Venus surface. After that TCM the radial component is 9.6 km (nominal swing-by altitude is 300 km).

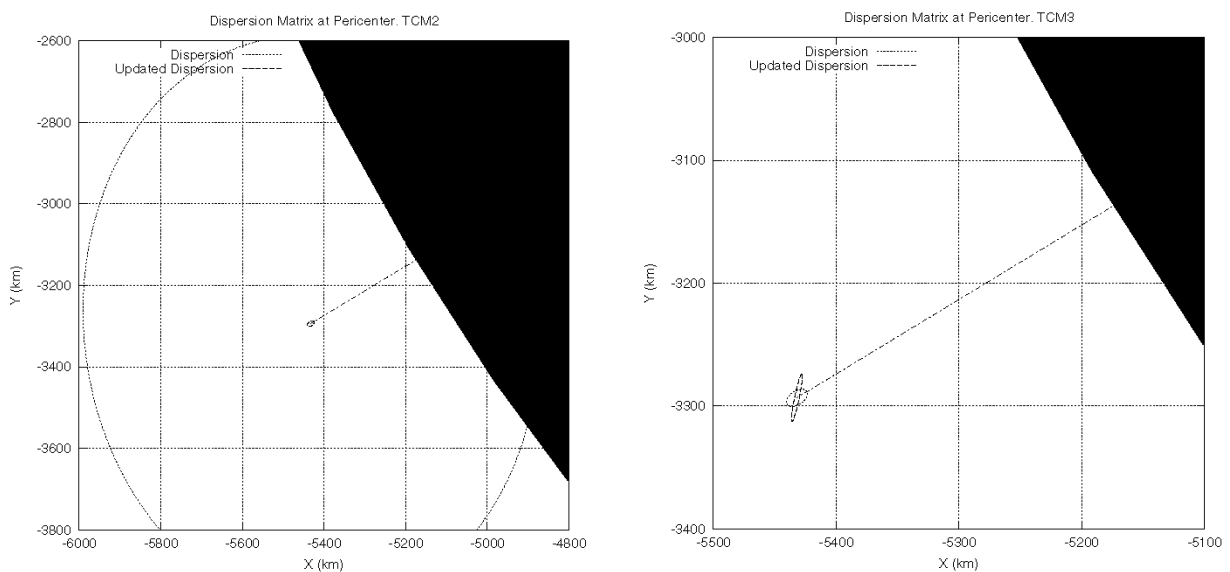


Figure 4-3. Dispersion 1σ ellipses at pericentre of the second Venus gravity assist (GAM V2).

The last TCM is useless, as it has been already mentioned. It can be seen on the right hand side Figure, where the radial error increases. It shows again that this TCM can be removed.

4.3.2 Navigation Between Second and Third Venus Swing-bys

For this arc, the solar radiation pressure is modelled as an exponentially correlated variable. The correlation time is taken equal to 10 days and the steady-state standard deviation to 0.5 % of the force coefficient $C_r S/m$.

Table 4-4 summarizes the estimates of the correction manoeuvres. The first TCM, that takes place 10 days after GAM V2, is supposed to clean up the errors of the swing-by analysed in the previous paragraph. From the table it is seen that this manoeuvre drives the ergol consumption for the whole arc, as it represents more than 95 % of the total consumption. The remaining corrections are a refinement of the targeting.

The 3σ propellant budget is roughly 14 m/s. Hence a conservative value lies between 15 m/s and 20 m/s.

Table 4-5 gives an overview of the achievable precision in the target plane taken at the pericentre of the hyperbola of Venus GAM V3. The size of the dispersion ellipse after TCM4 is sufficient (radial distance is 4.4 km). Hence there is no need for a fifth manoeuvre prior to GAM V3.

Correction manoeuvre	Day	Mean (m/s)	Δv (95%) (m/s)	Δv (99%) (m/s)	Max (m/s)
TCM1	GAM V2 + 10	5.64	10.78	13.44	20.56
TCM2	GAM V2 + 1 rev	0.17	0.35	0.44	0.67
TCM3	GAM V2 + 2 rev	0.04	0.09	0.12	0.19
TCM4	GAM V3 - 15	0.04	0.08	0.11	0.17

Table 4-4. Trajectory correction manoeuvres statistics between the second and the third Venus (GAM V3).

Correction manoeuvre	Day	SMAA (km)	SMIA (km)	q (deg)	LTF (s)	Radial (km)
(Initial)	GAM V2	184437	6041.8	-8.9	396.8	17959.0
TCM1	GAM V2 + 10	1937.6	88.6	-9.9	8.1	169.7
TCM2	GAM V2 + 1 rev	77.8	13.5	-14.1	0.3	13.6
TCM3	GAM V2 + 2 rev	46.5	4.5	20.8	0.8	27.2
TCM4	GAM V3 - 15	4.5	0.4	88.8	0.1	4.4

Table 4-5. Evolution of the 1σ dispersion covariance matrix at pericentre projected on the target plane (GAM V3).

Figure 4-4 and Figure 4-5 represent the evolution of the knowledge and dispersions of the velocity and the position before GAM V3. From these figures it is obvious that it not interesting to apply an additional manoeuvre after TCM4 if the knowledge is not improved by at least one order of magnitude.

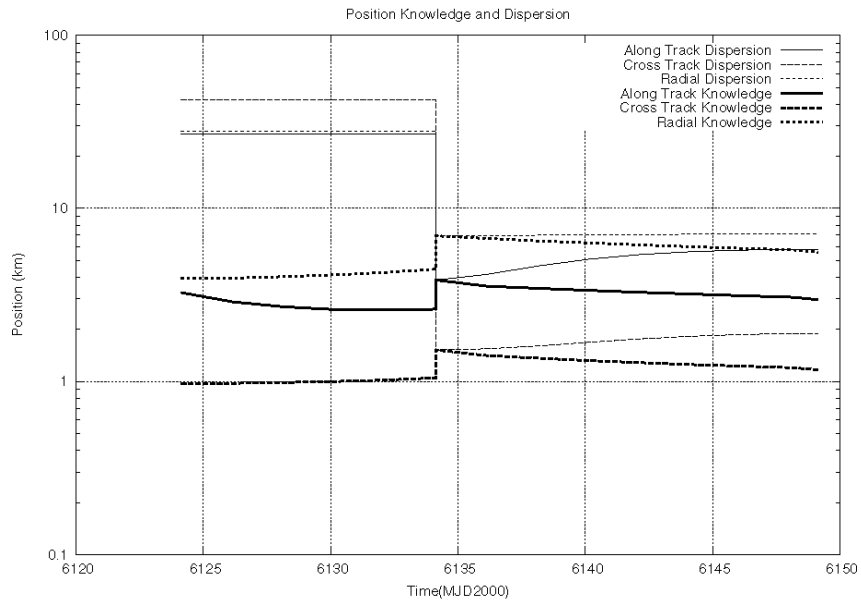


Figure 4-4. Evolution of the 1σ position knowledge (thick lines) and dispersion (thin lines) mapped to the pericentre (GAM V3).

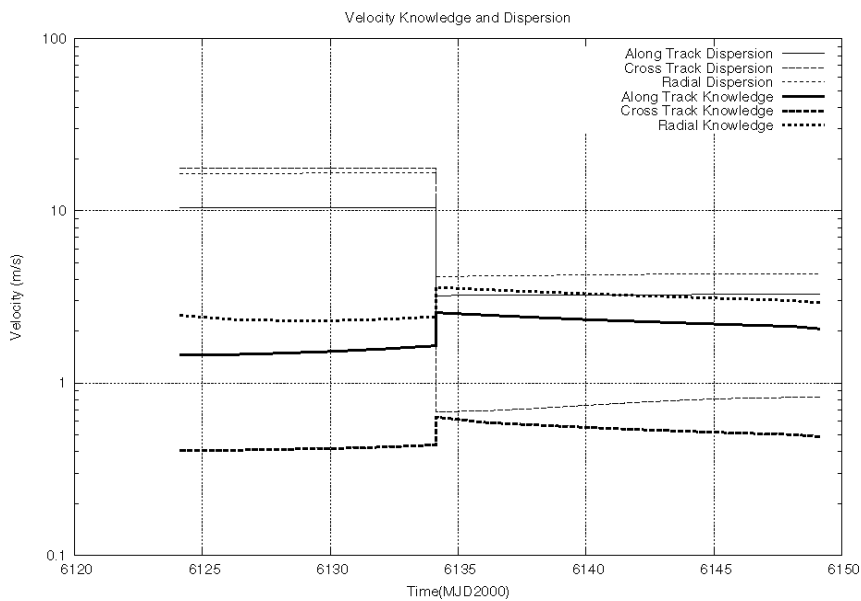


Figure 4-5. Evolution of the 1σ velocity knowledge (thick lines) and dispersion (thin lines) mapped to the pericentre (GAM V3).

The error ellipses at the pericentre before and after TCM4 are given in Figure 4-6.

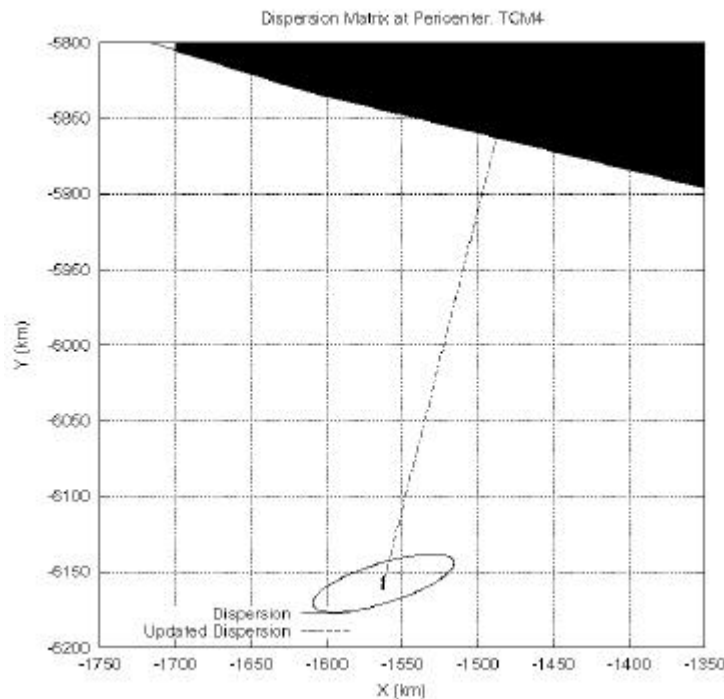


Figure 4-6. Dispersion σ ellipse at pericentre of the second Venus gravity assist (GAM V3).

4.4 Feasibility of the Manoeuvre Execution

In order to minimise spacecraft cost and complexity, a 4thrustrer configuration similar to Mars Express is selected for the Solar Orbiter, with thrusters implemented on the anti-Sun side of the spacecraft. As a consequence, prior to each trajectory manoeuvre, the spacecraft must be slewed for achieving the desired thrust direction. At close Sun distance, this direction may not be compatible with the spacecraft thermal design.

To cope with this thermal constraint any trajectory manoeuvre at a Sun distance below 0.6 AU is to be avoided.

For the 2013, 2015 and 2018 launches, none of the manoeuvres mentioned in this report violate this constraint.

For the 2017 launch, in contrast to the other launch years, all Venus GAM arrivals are inward. This makes the pre-swing-by manoeuvres critical.

Venus GAM 2: the first 103 days after Earth GAM 2 distance to Sun centre $r_S > 0.6$ AU. This is plenty of time to perform a good targeting for Venus GAM 2. Then follows a 53-day period when $r_S < 0.6$ AU and then only 12 days when $r_S > 0.6$ AU prior to Venus GAM 2. Swing-by adjustment and trimming has to be performed during these 12 days. This is just a bit short (2-week is recommended) but still feasible. However, this is a critical point for the 2017 launch.

Venus GAM > 2: all Venus arrivals are inward. However, the ballistic arc between two swing-by is three to four revolutions long, allowing a good estimation of the perturbation profile along the orbit and much flexibility in selecting manoeuvre times. The proposed strategy, consisting in performing targeting manoeuvres at crossing through Venus orbit, prevents the need of performing manoeuvres

when $r_S < 0.6$ AU. Before encounter there is a 12-day period when $r_S > 0.6$ AU, rather short but acceptable, knowing that targeting is very accurate on the resonant orbit.

4.5 Conclusion of the Navigation Analysis

A preliminary study on the Solar Orbiter navigation during the coast arcs preceding the second and the third Venus swing-by is presented. The following conclusions can be derived from the results obtained for the nominal scenario:

1. The estimation of this navigation *DV* budget is preliminary, due to the following reasons:
 - The size of the trajectory correction manoeuvres depends directly on the assumed initial dispersion in the velocity.
 - The guidance strategy used in this study is not necessarily optimal. In particular the sequence of TCMs chosen between GAM V2 and GAM V3 could be further improved.
 - For estimating the effect of radiation pressure perturbation a very conservative value for the area-to-mass ratio was taken.
2. Conservative values for the *DV* budget are:
 - 15 m/s for GAM V2.
 - 20 m/s for GAM V3 and following.
3. The simulations tend to show that the mission is safe: the \mathfrak{R} radial distances at the pericentre after the last TCM (40.2 km for GAM V2 and 4.4 km for GAM V3) are rather small compared with the altitude of the swing-bys (300 km).
4. Further studies should concentrate on the following points:
 - Parametric analyses to find the optimal guidance sequence (number and location of TCMs).
 - Improve the knowledge of the solar radiation pressure that is the main source for dispersions at the pericentre. Hence the error ellipse size for GAM V2 could be decreased and the amplitude of the first TCM after the swing-by could be reduced.

DV budget for the Venus GAM 3 is conservatively estimated here as 20 m/s. However, the 99-percentile figure is less than 15 m/s. Therefore, a global figure of 15 m/s per GAM for all GAM preparation/correction to be performed with monopropellant is proposed

With regard to the spacecraft thermal constraint that prevents manoeuvres to be performed when spacecraft is at a distance to the Sun inferior to 0.6 AU, all manoeuvres are checked to be performed outside this limit radius.

PAGE INTENTIONALLY LEFT BLANK

5. LAUNCHER'S PERFORMANCE

A Soyuz launcher with its Fregat upper stage is selected for the Solar Orbiter. Launch will be from Kourou. Starsem released basic information about Soyuz performance upgrade for escape missions during an ESA Horizons 2005-2012 Mission Status meeting (2002-02-27, Paris, Ref. 2). Improvement of the launch vehicle and its upper stage were described and a performance curve for escape mission in terms of the escape energy C_3 was given. This performance, updated at ESOC (Ref. 3), is shown on Figure 5-1. The mass of the adapter is included in the performance. The improved launcher (Soyuz/ST version 2-1b) will be available for launches from Kourou from 2008 on.

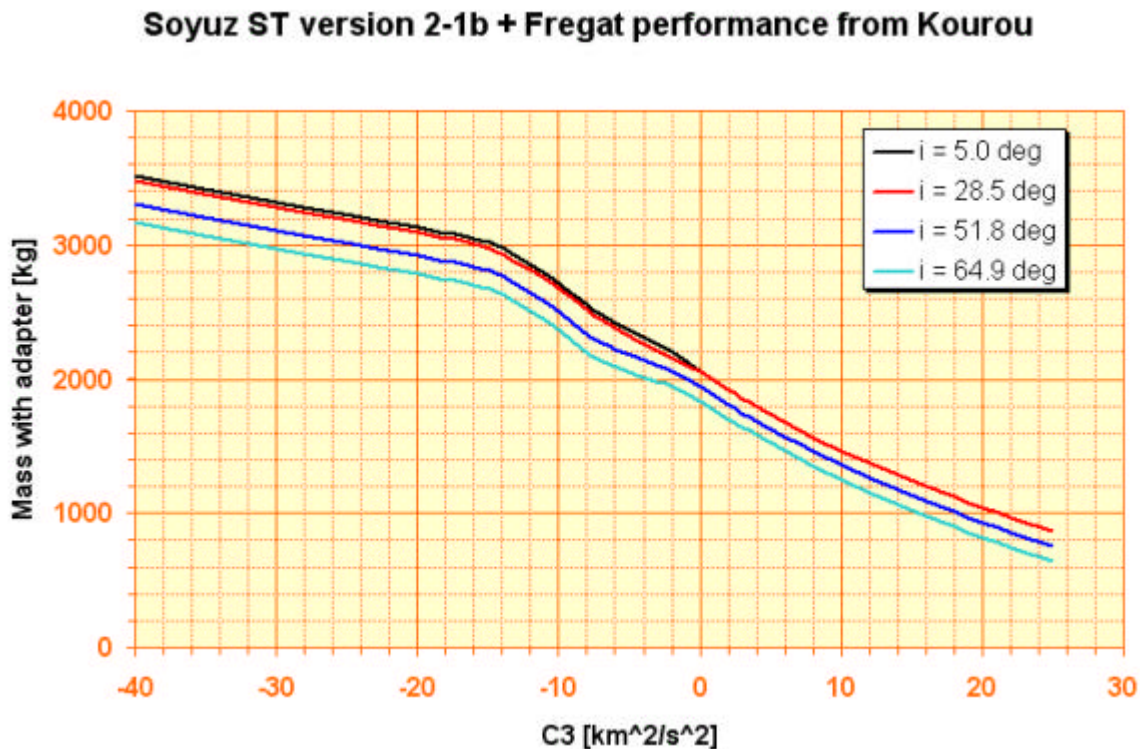


Figure 5-1. Soyuz/ST + Fregat performance (kg, including adapter) for highly elliptic (perigee height 200 km) and escape missions in terms of C_3 for a launch from Kourou with inclination $i = 5^\circ$, 28.5° , 51.8° and 64.9° (Ref. 3).

In a diagram payload mass versus C_3 the performance curve is nearly linear. By extending the line toward negative values of C_3 , performance for highly elliptic orbits can also be shown on the same diagram for a given perigee height h_p (usually 180-200 km). The relation between C_3 and apogee height h_a is the following

$$C_3 = -\frac{2m_E}{h_a + h_p + 2R_E}$$

where m_E is the Earth gravitational constant ($398600.448 \text{ km}^3/\text{s}^2$) and R_E the mean Earth equatorial radius (6378.14 km). Correspondence between C_3 and apogee height and also perigee injection DV is given in Figure 5-2.

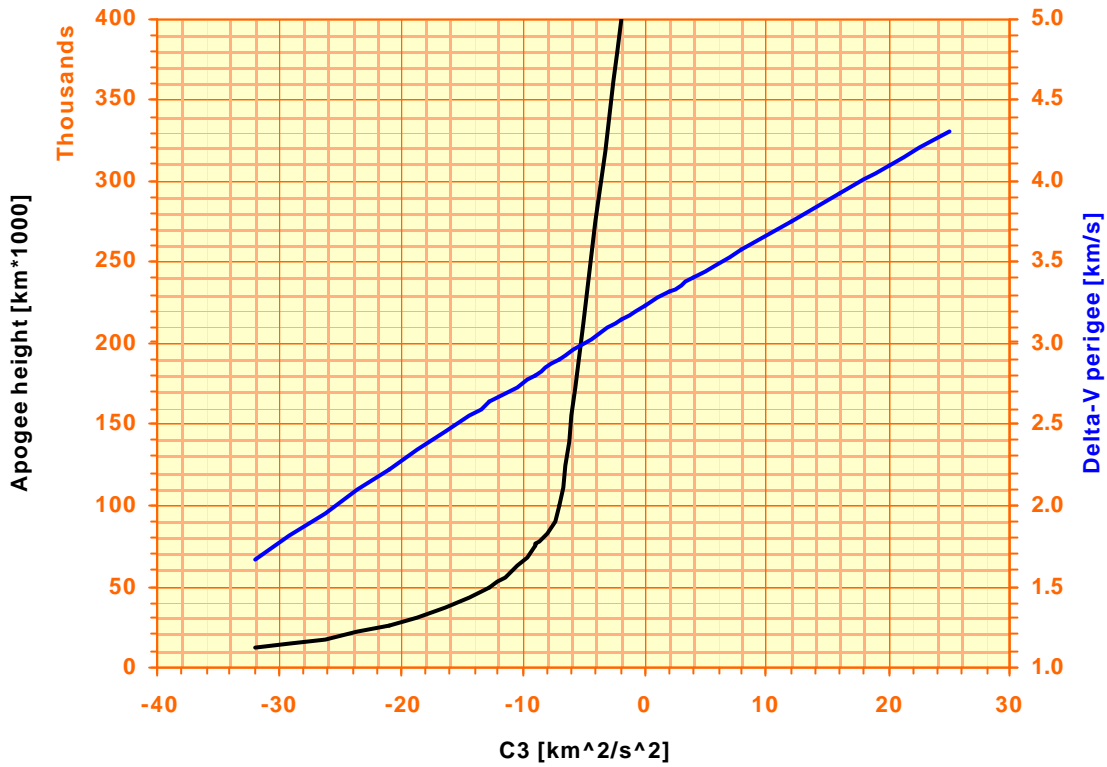


Figure 5-2. Correspondence between C_3 and apogee height (black curve) and perigee injection DV (blue curve).

Figure 5-1 includes performance curves for four inclinations (for elliptic orbit) or declination (for hyperbolic orbit). These curves are estimated through extrapolation of the currently best-known performance data available for Soyuz/ST.

According to a recent decision by Starsem, for all Soyuz launches from Kourou the launcher will be injected into a 180 km height circular parking orbit. After separation of the composite Fregat + payload from the launcher, the Fregat stage will be ignited when the proper asymptote declination can be reached. Declination from -30° to 30° can be achieved without performance penalty. This is reflected in Figure 5-1, where the declination 5° and 28.5° curves are superposed for $C_3 > 0$.

6. CONCLUSION

The Solar Orbiter mission is divided in three main parts:

1. Launch and initial part of transfer up to time when scientific instruments are operational
2. Science Phase, when basic scientific requirements for solar observation are satisfied
3. Extended mission, when the inclination of the orbit is further raised

The nominal mission is composed of the transfer and first part of Science Phase. During transfer, two types of manoeuvres are executed: Gravity Assist Manoeuvres through planetary encounters with Venus and Earth and Deep Space Manoeuvres through firing of a propulsion unit. Then, inclination is raised through a series of GAMs with Venus while orbiting on a 3:2 resonant orbit with Venus.

DSM can be achieved through impulsive thrust with a low specific impulse Chemical Propulsion unit. With a typical swing-by transfer sequence Venus – Earth – Earth – Venus, the duration of the transfer is about 3.5 years and the total DV is smaller than 0.25 km/s (for some launch opportunities, smaller than 100 m/s).

During the inclination increase phase of the mission, the orbit inclination is raised every three revolutions (450 days) by performing a Venus GAM. An inclination of 34° to 35° above the solar equator is reached after 4 to 5 of such encounters.

The end of the inclination raise period is part of the extended mission. The end of mission will be declared during the period following the last Venus GAM (no. 7), where the selected orbit will be non-resonant in order to prevent a possible crash on the planet during next Venus encounter.

Launcher foreseen for the Solar Orbiter is a Soyuz/ST version 2-1b with a Fregat upper stage launched from Kourou. Required escape velocity is between 3 and 4 km/s, leading to a launcher performance of 1500 to 1200 kg.

Launches in 2013, 2015, 2017 and 2018 were optimised, resulting in a satellite dry mass of 1028, 1124, 1172 and 1103 kg and a propellant consumption of 287, 180, 138 and 239 kg respectively.

The 2017 launch results in a less performant trajectory than for the other years. The transfer phase is longer by 9 months, the first resonant orbit after Venus GAM 2 has a perihelion radius of 0.28 AU and one has to wait three Venus years on this orbit before acquiring the baseline 3:2 resonant orbit with a 0.23 AU perihelion radius. As a result, the end of nominal mission is delayed by 16 months.

Finally, an analysis of the navigation tasks to be performed before and after the Venus GAMs during the Science phase shows that these manoeuvres can be performed by a 4-thruster AOCS at a cost of about 15 m/s per GAM. All manoeuvres can be performed at a distance to the Sun larger than 0.6 AU, where satellite thermal design can allow any direction for the manoeuvre.

PAGE INTENTIONALLY LEFT BLANK

7. REFERENCES

1. G Janin, Solar Orbiter Phase A Mission Analysis Input, MAO WP-472, Issue 1.1, ESA-ESOC, April 2004.
2. Soyuz for Exploration Missions, Presentation to ESA/Astrium, *Meeting ESA Horizons Mission Status 2005-2012 and Soyuz*, ESA-HQ, Paris, 2002 February 27.
3. A Yáñez & M Hechler, Soyuz/Fregat from Kourou: Estimated Performances for HEO and Escape Missions (Draft), *MAO WP-470*, ESA-ESOC, 2004-03-30.